Journal of Medicinal Chemistry

pubs.acs.org/jmc Article

Antiarrhythmic Hit to Lead Refinement in a Dish Using Patient-Derived iPSC Cardiomyocytes

John R. Cashman,* Daniel Ryan, Wesley L. McKeithan, Karl Okolotowicz, Jorge Gomez-Galeno, Mark Johnson, Kevin J. Sampson, Robert S. Kass, Arash Pezhouman, Hrayr S. Karagueuzian, and Mark Mercola

Cite This: *J. Med. Chem.* 2021, 64, 5384−5403 Read Online

ACCESS | Metrics & More | Article Recommendations | Supporting Information

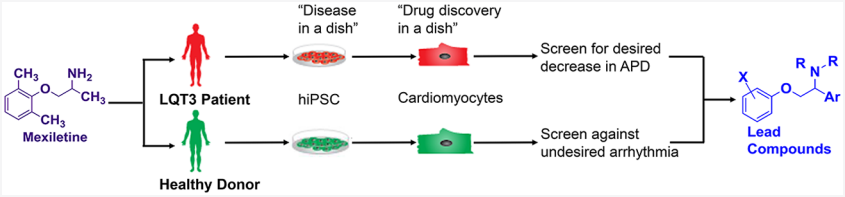

ABSTRACT: Ventricular cardiac arrhythmia (VA) arises in acquired or congenital heart disease. Long QT syndrome type-3 (LQT3) is a congenital form of VA caused by cardiac sodium channel (I_{NaL}) SCN5A mutations that prolongs cardiac action potential (AP) and enhances I_{NaL} current. Mexiletine inhibits I_{NaL} and shortens the QT interval in LQT3 patients. Above therapeutic doses, mexiletine prolongs the cardiac AP. We explored structure−activity relationships (SAR) for AP shortening and prolongation using dynamic medicinal chemistry and AP kinetics in human-induced pluripotent stem cell-derived cardiomyocytes (hiPSC-CMs). Using patient-derived LQT3 and healthy hiPSC-CMs, we resolved distinct SAR for AP shortening and prolongation effects in mexiletine analogues and synthesized new analogues with enhanced potency and selectivity for I_{NaL}. This resulted in compounds with decreased AP prolongation effects, increased metabolic stability, increased I_{NaL} selectivity, and decreased avidity for the potassium channel. This study highlights using hiPSC-CMs to guide medicinal chemistry and "drug development in a dish".

INTRODUCTION

Approximately one million individuals are hospitalized every year for arrhythmias in the United States, making arrhythmias one of the top causes of healthcare expenditures with a direct cost of almost $50 billion annually for diagnosis, treatment, and rehabilitation.[1] Another 300,000 individuals die of sudden arrhythmic death syndrome every year.[2] Arrhythmias are very common in older adults, but unfortunately, drugs used to treat arrhythmias have liabilities. In addition, numerous drugs have been withdrawn from the market because they induce QT prolongation (Figure 1) and a potentially fatal ventricular tachycardia (VT), torsade de pointes (TdP) (Figure 2).[3]

Cardiac sodium current (I_{NaP}) occurs in less than a millisecond and underlies the rapid upstroke or phase 0 of the AP (action potential) (Figure 1). Thereafter, an activation gate and an inactivation gate on the sodium channel are both open. After several milliseconds, the current begins to decay, contributing to a notch in the AP called phase 1. At this point, some of the channels are inactivated (shown as "I" with the inactivation gate closed). There is no commonly accepted name for this phase of I_{Na}, but here, it is labeled "early I_{Na}" (Figure 1). After several milliseconds, I_{Na} normally decays to <1% of I_{NaP}, but a residual current flows as late I_{NaL} and this depolarizing current along with calcium currents support phase 2 or the plateau of the AP. The mechanisms for I_{NaL} at the

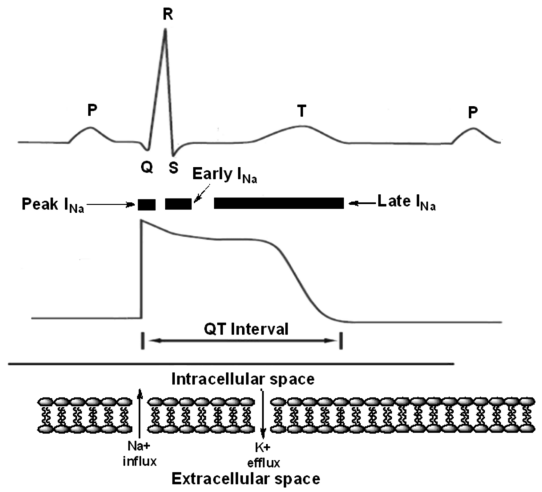

Figure 1. Schematic representation of cardiac cell membrane action potential (AP) and its relation with surface electrocardiogram.

Received: September 3, 2020
Published: May 4, 2021

https://doi.org/10.1021/acs.jmedchem.0c01545
J. Med. Chem. 2021, 64, 5384−5403

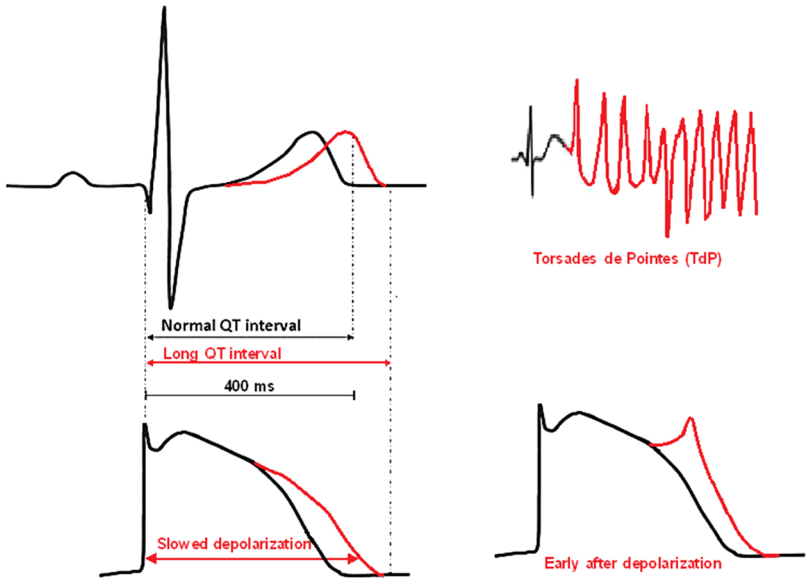

Figure 2. Effect of slow membrane depolarization on the QT interval on a surface electrocardiogram.

sodium current level are multiple but can generally be thought of as incomplete inactivation. Eventually, activating potassium currents repolarize the membrane (phase 3 of the AP), and when the voltage decreases below the sodium channel threshold, the activation gate closes.

Mexiletine is an orally available inhibitor of muscles and neuronal sodium channels and is a class 1B antiarrhythmic drug in the Vaughan–Williams classification scheme.[4] Mexiletine has been used to treat life-threatening ventricular arrhythmia and also long QT syndrome type 3 (LQT3).[5,6] Cardiac AP is initiated by the opening of the cardiac sodium channel $Na_v1.5$ (encoded by *SCN5A*) conducting the large peak sodium current (I_{NaP}) responsible for the AP upstroke. In healthy individuals, the sodium channels inactivate with depolarization. However, LQT3 causal mutations in $Na_v1.5$ impair channel inactivation and accelerate recovery from the inactivated state.[7−9] Increased I_{NaL} opposes repolarization and prolongs the AP, thus prolonging the QT interval on the surface electrocardiogram.[7,10] Mexiletine inhibits I_{NaL} and consequently shortens the QT interval in LQT3 patients[11] and decreases their risk of developing ventricular tachycardia and ventricular fibrillation.[12] However, at concentrations slightly greater than its therapeutic plasma concentration and IC_{50} for inhibition of I_{NaL}, mexiletine also prolongs the cardiac AP and promotes potentially proarrhythmic events (including early after depolarizations (EADs)) *in vitro*.[13,14] Observations of proarrhythmia have restricted mexiletine use although cardiologists generally predetermine a safe and efficacious dose. Mexiletine has liabilities. The FDA-approved label states that severe liver injury and blood dyscrasias (i.e., leukopenia or agranulocytosis) and other adverse reactions including reversible gastrointestinal and nervous system problems have been reported after mexiletine treatment. Mexiletine also has a relatively short half-life (i.e., $t_{1/2}$ α-phase 3−12 min and β-phase 6−12 h[15]) that necessitates multiple doses per day. Greater doses of mexiletine produce side effects in the central nervous system.[16] Accordingly, mexiletine analogues were designed to replace metabolically labile groups with metabolically stable moieties to increase bioavailability, decrease the dose, and improve the therapeutic-to-toxicity ratio.

Given that these latter properties are potentially proarrhythmic, it is important to determine if they are mediated by distinct determinants in the chemical structure of mexiletine as those responsible for the desirable inhibition of I_{NaL} and whether structure modifications might decrease the AP prolonging effects, increase metabolic stability (and decrease the required dose), and increase selectivity for the sodium channel, thus decreasing avidity for the potassium channel and decrease toxicity.

Herein, we report the application of human-induced pluripotent stem cell-derived cardiomyocytes (hiPSC-CMs) to comprehensively evaluate proarrhythmic effects of mexiletine analogues and define chemical determinants responsible for antiarrhythmia. We used patient-derived hiPSC-CMs carrying a previously described LQT3 mutation in *SCN5A* (F1473C)[17] to quantify the extent of AP shortening of mexiletine and analogues. LQT3 human CMs were used to determine the mexiletine analogue's beneficial effects, quantified as the EC_{50} for shortening the APD, a fold shortening of the APD, and a concentration that caused shortening of the action potential. These results were compared to the concentration of a test compound required for cessation of cell beating, an EC_{50} for shortening the APD, and fold shortening of the APD in normal cardiomyocytes. Both normal and patient-derived LQT-3 hiPSC-CMs were previously characterized for the effects of benchmark reference drugs on AP kinetics and arrhythmia.[13]

To quantify the effect of chemical structural modification on the CM response, each test compound was tested in a dose–response study (i.e., 0−200 μM, nine concentrations, in triplicate) to identify the concentration of cessation of cell beating, determine the concentration at which EADs occurred, and quantify the EC_{50} for prolonging the APD.

Optical recordings of AP kinetics[13] were used as the primary assay, and results were confirmed by automated patch clamp recording[17] of exogenously expressed *SCN5A* variants as a secondary assay. Based on results for AP kinetics, inhibition of I_{NaL} and I_{NaP}, and blockade of the potassium current I_{Kr} (i.e., hERG) that mediates the repolarizing potassium current, a SAR arose for the mexiletine analogues synthesized and tested.

https://doi.org/10.1021/acs.jmedchem.0c01545
J. Med. Chem. 2021, 64, 5384−5403

The results led to identification of significantly more potent and selective I_{NaL} inhibitors with decreased proarrhythmic effects and much improved physicochemical properties. Compounds **30**, **33**, **39**, and **62** were shown to be effective antiarrhythmic compounds in hiPSC-CM models of LQT3-associated arrhythmia.

Scheme 1. Regions of Mexiletine Modified to Lead to Greater Potency, Selectivity, and Less Toxicity. Region I (red) Is Alpha to the Amine, Region II (Green) Is the Phenoxy Moiety, and Region III (Blue) Contained N-Substituents

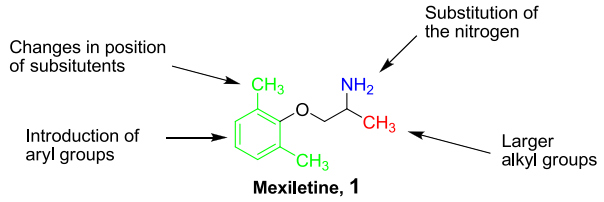

RESULTS

Chemistry. Mexiletine and analogues were prepared using the synthetic routes described in Scheme 2. Some synthetic procedures were adapted from literature reports.[18,19] Mexiletine was divided into three hypothetical regions for theoretical molecular dissection as follows: Region I included substituents α to the amine, Region II included substituents associated with the phenoxy moiety, and Region III included *N*-substituents. In a typical synthesis, substituted phenols were combined with α-bromoketones in the presence of potassium carbonate to afford phenoxy alkyl ketones.[20] α-Aryloxy ketones with variable substituents[21] were the precursors for one of the two synthetic routes. To prepare primary amines, a two-step protocol was employed that involved preparation of benzyl oximes and their subsequent reduction with borane to give the desired amines (**2**–**42**).

Scheme 2. General Synthesis of Mexiletine Analogues and *N*-Substituted Mexiletine Analogues[a]

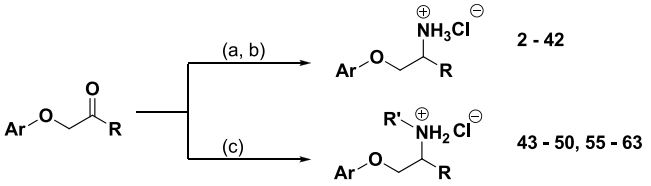

[a](a) $PhCH_2ONH_2$-HCl, pyridine, ethanol, 21 °C. (b) BH_3-THF, 65 °C, followed by treatment with HCl-ether. (c) *R*′-NH_2, $NaBH_3CN$, ethanol, 21 °C, followed by treatment with HCl-ether.

Secondary racemic amines were directly prepared by a one-step reductive amination procedure to give *N*-substituted products **43**–**50** and **55**–**63** as reported.[22] *N*-Acylated analogues **51**–**54** were generated from the corresponding primary amines by treatment with either acetyl chloride or benzoyl chloride in the presence of triethylamine. Chiral analogues were generated by the method illustrated in Scheme 3 for (*R*)-**30** and (*R*)-**59**. Chiral *N*-acylated 4-phenyl 1,2,3-oxathiazolidine-2,2-dioxide derivatives were combined with substituted phenols under basic conditions.[23] To convert to the primary amines, the *N*-acyl group used was a *t*-Boc substituent that was removed under acidic conditions. For the methoxyethyl-substituted amine **59**, an *N*-methoxy acetyl protecting group was reduced with lithium aluminum hydride and afforded the secondary amine (Scheme 3).

The hydrochloride salts of the amine products were used for biological testing and judged to be greater than 95% pure by ^{1}H NMR and HPLC.

BIOLOGICAL RESULTS

Effect of Mexiletine Analogues on Human Cardiomyocytes. Mexiletine, **1** was re-engineered by chemical synthesis to afford analogues with increased on-target potency (i.e., sodium channel) and decreased off-target (i.e., potassium channel) effects. The structure–activity relationship (SAR) for the effect of mexiletine analogues on normal and patient-derived hiPSC-CMs was systematically evaluated in CMs derived from an LQT3 patient (i.e., carrying the SCN5A F1473 mutation) and from an unrelated healthy donor. Thus, the effects of mexiletine analogues on CMs with channelopathies (i.e., disease in a dish) were compared to the effects of compounds on normal nonpathogenic CMs. To quantify the effect of modification of **1**, the molecule was conceptually divided into three exploratory regions (Scheme 1): (I) the region alpha to the primary amine moiety (red), (II) the phenoxy region (green), and (III) the *N*-substituted region (blue). Each compound was tested in a dose–response study (i.e., 0–200 μM, nine concentrations, in triplicate) in LQT3 hiPSC-CMs to determine a concentration of cessation of cell beating, an EC_{50} for shortening the APD, a fold shortening of the APD, and a concentration that caused shortening of the AP. In normal cardiomyocytes, the concentration that caused cessation of cell beating, the concentration that caused proarrhythmic induction of EADs, and the EC_{50} for shortening the APD were determined. These latter measures were indices of cell toxicity.

Initially, a small group of approximately 20 compounds directed at structural modifications of the portion of **1** alpha to the primary amine (i.e., Region I) were synthesized and tested

Scheme 3. Syntheses of Chiral Analogues (*R*)-30 and (*R*)-59[a]

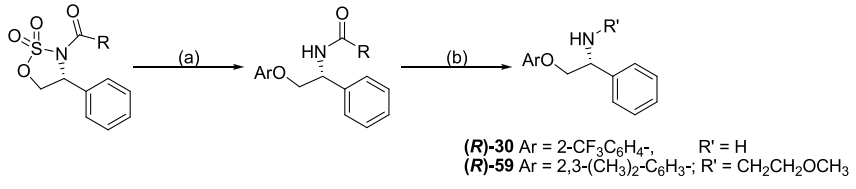

[a](a) 2-Trifluoromethylphenol (for (*R*)-**30**, R = *tert*-BuO–) or 2,3-dimethylphenol (for (*R*)-**59**, R = CH_2OCH_3), NaH, DMF, 21 °C, 16 h. (b) For (*R*)-**30**: HCl, methanol, 21 °C, 16 h. For (*R*)-**59**: $LiAlH_4$, THF, 75 °C, 16 h.

https://doi.org/10.1021/acs.jmedchem.0c01545
J. Med. Chem. 2021, 64, 5384–5403

Table 1. Effect of Alpha Substituents of Mexiletine on Cardiovascular Properties in Human iPSC-Derived Cardiomyocytes[a]

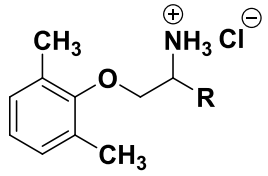

		LQT3 Cells				Normal Cells		
Number	R	Cessation Dose[b] (μM)	EC_{50} Shortening[c] (μM)	Fold-Shortening[d]	Maximal Shortening Dose[e] (μM)	Cessation Dose[b] (μM)	EAD Dose[f] (μM)	EC_{50} Prolongation[g] (μM)
1		-	1.8	1.335	22	-	200	20.4
2		22	< 0.8	1.182	2.5	-	7.4	-
3		200	0.8	1.162	22	-	66	8.0
4		66	< 0.8	1.136	0.8	66	-	-
5		66	< 0.8	1.174	2.5	133	-	4.0
6		66	-	1.588	22	66	-	-
7		66	1.4	1.480	22	66	-	-
8		66	-	1.425	7.4	66	-	-
9		133	4.73	1.309	22	-	-	-

[a]Kinetic imaging cytometer assay results for alpha-substituted mexiletine derivatives. [b]Lowest dose that cessation of beating was observed. [c]EC_{50} for shortening the AP. [d]Ratio of AP untreated/AP treated. [e]Maximal dose that shortens the AP. [f]Dose that early after depolarization was observed. [g]EC_{50} for prolongation of the AP. The symbol "-" denotes that the indicated effect was not observed. EAD dose indicates the concentration at which the compound induced early after depolarizations.

(Tables 1 and 2). The results of these studies showed that an alpha aryl moiety showed greater fold shortening than aliphatic substituents. However, partial aryl characters (i.e., cyclopropyl compounds) (Table 2) were less effective at fold shortening than aryl compounds. Modifications of the phenoxy moiety (Tables 3 and 4) (i.e., Region II) resulted in compounds with potent APD shortening. *N*-Modification of selected compounds (Tables 5 and 6, Region III) yielded additional derivatives with potent fold shortening and in some cases less toxicity to normal CMs.

LQT3 patient-derived hiPSC-CMs were resistant to the adverse effects of mexiletine, suggestive of the previously reported patient that tolerated a high dose.[17] Therefore, the detrimental effects on AP prolongation and EADs were most apparent in healthy normal donor hiPSC-CMs. Thus, the results from studies with normal CMs served as a control and an indicator of toxicity of compounds tested. In addition to measuring desired APD shortening in LQT3 cardiomyocytes and undesired APD prolongation and EADs in normal cardiomyocytes, on-target potency for inward sodium late currents (I_{NaL}), selectivity for I_{NaL} versus I_{NaP}, and selectivity against potassium currents (I_{Kr}) were obtained with whole cell automated planar patch clamp studies in which the SCN5A and hERG channels were expressed in CHO cells.

Region I. Analogues of Mexiletine. In LQT3 hiPSC-CMs, compared to mexiletine, **1**, *tert*-butyl, cyclopropyl, and cyclohexyl analogues (i.e., **2**, **3**, and **4**) were about 12−15% less potent at shortening the APD (Table 1). In contrast, aryl-substituted derivatives, 4-methyl phenyl, 4-CF_3 phenyl, and 4-methoxy phenyl (i.e., **6**, **7**, and **8**) were about 7−19% more potent than mexiletine at shortening the APD. The naphthyl derivative, compound **9**, was about as potent as mexiletine at shortening the APD. In contrast, in normal hiPSC-CMs, compounds **1**−**9** did not cause detectable shortening of the APD.

Mexiletine did not cause cessation of cell beating in either LQT3 or normal hiPSC-CMs but induced EADs at 200 μM in normal cells in primary screening (Table 1). Cessation of beating is an indication of cardiotoxicity, and EADs are indicative of proarrhythmic activity for a compound. Compounds **2** and **3** induced EADs at 7.4 and 66 μM, respectively, in normal CMs. Of the alpha amine-substituted compounds examined, cessation of beating was observed (i.e., 66−133 μM range) but the cyclopropyl derivative (i.e., **3**) was less potent and less toxic.

https://doi.org/10.1021/acs.jmedchem.0c01545
J. Med. Chem. 2021, 64, 5384−5403

Table 2. Effect of Phenoxy Substituents of Alpha Cyclopropane Mexiletine Analogues on Cardiovascular Properties in Human iPSC-Derived Cardiomyocytes[a]

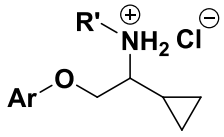

		LQT3 Cells				Normal Cells		
Number	Ar and R'	Cessation Dose[b] (μM)	EC_{50} Shortening[c] (μM)	Fold-Shortening[d]	Maximal Shortening Dose[e] (μM)	Cessation Dose[b] (μM)	EAD Dose[f] (μM)	Fold-Prolongation[g]
1	Mexiletine	-	1.83	1.335	22	-	66	2.262
10	(*R*)-Mexiletine	-	0.96	1.346	7.4	-	200	2.661
11	(*S*)-Mexiletine	-	0.8	1.25	22	-	200	2.289
12	Ar = 	200	0.8	1.162	22	200	66	2.805
13	Ar = 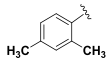 R' = H	200	1.36	1.119	66	200	66	2.12
14	Ar =  R' = H	200	-	1.18	22	66	-	-
15	Ar =  R' = $CH_2CH_2OCH_3$	200	0.022	1.11	66	200	66	1.686
16	Ar =  R' = H	200	2.06	1.15	22	200	66	2.12

[a]Kinetic imaging cytometer assay results for alpha cyclopropane mexiletine derivatives. [b]Lowest dose that cessation of beating was observed. [c]EC_{50} for shortening the AP. [d]Ratio of AP untreated/AP treated. [e]Maximal dose that shortens the AP. [f]Dose that early after depolarization was observed. [g]EC_{50} for prolongation of the AP. The symbol "-" denotes that the indicated effect was not observed.

Generally, the potency for shortening the APD (i.e., EC_{50} for shortening) did not exactly correspond to the potency of the concentration causing fold shortening of the APD in LQT3 cardiomyocytes (Table 1) although compounds **2** (isopropyl), **4** (cyclohexyl), and **5** (phenyl) were similarly potent at both measures based on the lack of potency of cessation of beating. Based on the potency of shortening by cyclopropyl compound **3**, additional cyclopropyl derivatives were synthesized and tested (Table 2).

Like mexiletine or its individual enantiomers, the cyclopropyl-substituted compounds in this class (i.e., compounds **12**, **13**, **15**, and **16**) only caused cessation of cell beating at 200 μM or not at all in either LQT3 or normal CMs. Compound **14** caused cessation of cell beating at 66 μM and was not extensively examined further. However, compounds **12**, **13**, **15**, and **16** did induce EADs at 66 μM in normal CMs and were deemed to possess some potential for toxicity (Table 2).

In contrast to mexiletine or its stereoisomers, for this class of cyclopropyl mexiletine analogues, the potency for fold shortening the APD (i.e., EC_{50} for shortening) corresponded to the potency of the concentration causing shortening of the APD in LQT3 CMs (Table 2).

However, based on the potency that these cyclopropyl analogues caused toxic EADs at relatively low concentrations (i.e., 66 μM), additional cyclopropyl derivatives were not synthesized and tested. Rather, exploration of the phenoxy portion of the molecule was investigated to determine substituents that would afford less toxicity (i.e., cessation of beating, APD prolongation, and EADs).

Region II. Effect of Phenoxy Substituents on Mexiletine and Phenyl Mexiletine Analogues. Table 3 shows the results of modifying the phenoxy portion of mexiletine to afford analogues. In LQT3 CMs, compared to mexiletine, **1**, *ortho* monosubstituted methyl-, ethyl-, or propyl-

https://doi.org/10.1021/acs.jmedchem.0c01545
J. Med. Chem. 2021, 64, 5384−5403

Table 3. Effect of Phenoxy-Substituted Mexiletine Analogues on Cardiovascular Properties in Human iPSC-Derived Cardiomyocytes[a]

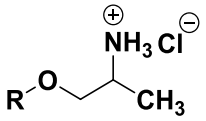

		LQT3 Cells				Normal Cells		
Number	R =	Cessation Dose[b] (μM)	EC_{50} Shortening[c] (μM)	Fold-Shortening[d]	Maximal Shortening Dose[e] (μM)	Cessation Dose[b] (μM)	EAD Dose[f] (μM)	EC_{50} Prolongation[g] (μM)
1		-	1.8	1.335	22	-	200	20.4
17		-	< 0.8	1.284	22	-	200	83.9
18		-	6.0	1.118	22	-	-	23.5
19		133	0.9	1.192	7.4	200	-	7.8
20		-	-	1.375	133	-	-	-
21		-	-	-	-	-	133	97.8
22		-	-	1.418	200	-	66	27.3
23		200	31.3	1.661	133	200	-	-
24		200	4.5	1.232	66	-	-	7.7
25		66	0.9	1.200	7.4	133	-	-

[a]Kinetic imaging cytometer assay results for phenoxy-substituted mexiletine derivatives. [b]Lowest dose that cessation of beating was observed. [c]EC_{50} for shortening the AP. [d]Ratio of AP untreated/AP treated. [e]Maximal dose that shortens the AP. [f]Dose that early after depolarization was observed. [g]EC_{50} for prolongation of the AP. The symbol "-" denotes that the indicated effect was not observed.

substituted compounds (i.e., **17**, **18**, and **19**) were less potent at shortening the APD based on fold shortening. In contrast, phenoxy-substituted derivatives, 2-CF_3, 3-CH_3, and 3-CF_3 (i.e., **20**, **22**, and **23**, respectively) were about 4−24% more potent than mexiletine at shortening the APD. The 3,5-disubstituted derivatives, compounds **24** and **25**, were slightly less potent than mexiletine at shortening the APD. In contrast, in normal CMs, compounds **17**−**26** did not cause detectable shortening of the APD and in some cases (i.e., compounds **19** and **24**) caused prolongation of the APD at relatively low concentrations.

Except compound **25** (i.e., at 66 μM) and compounds **19**, **23**, and **24** (at elevated doses), compounds in this class did not cause cessation of cell beating in either LQT3 or normal CMs. Compound **22** induced EADs at 66 μM. However, it required high concentrations (133−200 μM) to induce EADs in normal CMs for compound **17**, **21**, or **26** (Table 3).

As observed for chemotypes described above, generally, the potency for shortening the APD (i.e., EC_{50} for shortening) did not exactly correspond to the potency of the concentration causing fold shortening of the APD in LQT3 CMs (Table 3). However, compound **19** was potent at both measures. Based on the increase in potency of shortening the APD by certain monosubstituted phenoxy derivatives of mexiletine, additional analogues combining beneficial properties of the phenoxy ring and aryl substituent alpha to the amine were synthesized and tested.

Effect of Phenoxy Substituents on Alpha Phenyl Mexiletine Analogues. Because certain phenoxy-substituted mexiletine compounds and certain alpha amino aryl mexiletine analogues showed potency at shortening the APD, synthesis and testing of compounds that combined those two moieties were undertaken. Compared to the alpha amino phenyl analogue of mexiletine, certain phenoxy-substituted alpha amino phenyl derivatives potently increased fold shortening of the APD (Table 4). In LQT3 CMs, compared to phenyl mexiletine, **5**, *ortho* monosubstituted methyl-, ethyl-, or propyl-substituted compounds (i.e., **27**, **28**, and **29**) were more potent at shortening the APD by 37, 69, and 13%, respectively. Compared to phenyl mexiletine, 2-CF_3, 2-OCH_3, and 2-*O*-methoxy-CF_3, 2-*O*-CF_3 (i.e., **30**, **31**, and **32** and **33**, respectively) were 52, 26, 29, and 21% more potent at

https://doi.org/10.1021/acs.jmedchem.0c01545
J. Med. Chem. 2021, 64, 5384−5403

Table 4. Effect of Phenoxy Substituents of Alpha Phenyl Mexiletine Analogues on Cardiovascular Properties in Human iPSC-Derived Cardiomyocytes[a]

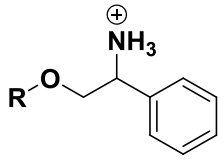

		LQT3 Cells				Normal Cells		
Number	R =	Cessation Dose[b] (μM)	EC_{50} Shortening[c] (μM)	Fold-Shortening[d]	Maximal Shortening Dose[e] (μM)	Cessation Dose[b] (μM)	EAD Dose[f] (μM)	EC_{50} Prolongation[g] (μM)
26		66	< 0.8	1.174	2.5	133	-	4.0
27		66	< 0.8	1.606	22	133	-	-
28		22	< 0.8	1.979	7.4	66	-	-
29	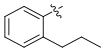	22	< 0.8	1.321	2.5	22	-	-
30		66	< 0.8	1.783	22	66	-	-
31		133	< 0.8	1.482	0.8	22	7.4	32.2
32	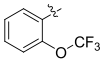	66	2.6	1.513	22	66	-	-
33	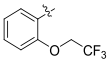	66	0.9	1.409	22	66	-	-
34		66	< 0.8	1.410	22	133	-	-
35		66	4.1	1.539	22	66	-	-
36		66	< 0.8	1.279	7.4	66	-	-
37		66	23.1	1.208	22	133	-	-
38		66	-	1.406	22	133	-	-
39		66	0.5	1.192	7.4	66	-	-
40		66	-	1.370	22	66	-	-
41		133	8.7	1.459	2.5	-	-	-
42		66	0.82	1.316	66	-	-	-

[a]Kinetic imaging cytometer assay results for phenyl mexiletine derivatives. [b]Lowest dose that cessation of beating was observed. [c]EC_{50} for shortening the AP. [d]Ratio of AP untreated/AP treated. [e]Maximal dose that shortens the AP. [f]Dose that early after depolarization was observed. [g]EC_{50} for prolongation of the AP. The symbol "-" denotes that the indicated effect was not observed.

https://doi.org/10.1021/acs.jmedchem.0c01545
J. Med. Chem. 2021, 64, 5384−5403

Table 5. Effect of *N*-Substituted Mexiletine Analogues on Cardiovascular Properties in Human iPSC-Derived Cardiomyocytes[a]

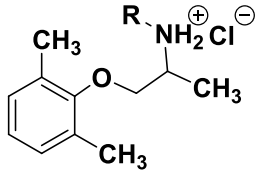

		LQT3 cells				Normal cells		
Number	R =	Cessation dose (μM)[b]	EC_{50} shortening (μM)[c]	Fold shortening[d]	Maximal shortening dose (μM)[e]	Cessation dose (μM)[b]	EAD dose (μM)[f]	EC_{50} prolongation (μM)[g]
1	H	-	1.8	1.335	22	-	200	20.4
43	Methyl	133	1.5	1.112	22	66	22	7.8
44	Ethyl	-	-	-	-	-	133	21.5
45	1-Propyl	200	-	1.199	2.5	200	66	10.4
46	1-Butyl	66	<0.8	1.180	2.5	133	66	7.8
47	2-Methoxyethyl	-	2.3	1.267	7.4	-	66	32.0
48	Phenyl	-	-	-	-	-	-	-
49	Benzyl	133	-	1.264	22	200	-	5.7
50	2-Phenylethyl	7.4	-	1.706	2.5	133	22	2.5
51	Acetyl	-	-	-	-	-	-	-
52	Benzoyl	133	57.82	1.45	66	66	-	-

[a]Kinetic imaging cytometer assay results for *N*-modified mexiletine derivatives. [b]Lowest dose that cessation of beating was observed. [c]EC_{50} for shortening the AP. [d]Ratio of AP untreated/AP treated. [e]Maximal dose that shortens the AP. [f]Dose that early after depolarization was observed. [g]EC_{50} for prolongation of the AP. The symbol "-" denotes that the indicated effect was not observed.

shortening the APD. The 3-substituted derivatives (i.e., compounds **34**–**38**) were slightly more potent than phenyl mexiletine at shortening the APD (i.e., 3–31%). Compared to phenyl mexiletine, compounds containing 4-substituted groups (i.e., **39** and **40**) increased shortening of the APD 2 and 17%, respectively. 1- and 2-Naphthyl derivatives of phenyl mexiletine increased shortening 12 and 25%, respectively, compared to phenyl mexiletine. In contrast, in normal CMs, compounds **5**–**42** did not cause detectable shortening of the APD and in some cases (i.e., compounds **5** and **31**) caused prolongation of the APD at relatively low concentrations.

Except compounds **41** and **42**, phenoxy-substituted derivatives of phenyl mexiletine (i.e., **27**–**40**) caused cessation of cell beating in both LQT3 and normal CMs (albeit at elevated concentrations). Compound **31** induced EADs at a relatively low concentration (i.e., 7.4 μM) in normal CMs (Table 4).

As a chemotype, generally, the phenoxy-substituted phenyl mexiletine analogues examined possessed great potency for shortening the APD (i.e., EC_{50} for shortening) and most were in the 0.8 μM or lower range in LQT3 CMs (Table 4). Based on the increase in potency of shortening the APD by certain monosubstituted phenoxy derivatives of phenyl mexiletine, additional derivatives combining beneficial properties of the phenoxy ring substituents and the amine nitrogen were synthesized and tested.

Region III. *N*-Substituted Analogues of Mexiletine. The effect of *N*-substitution on the pharmacological properties of mexiletine was investigated. Compared to mexiletine, most *N*-substituted mexiletine derivatives examined decreased the shortening dose of the APD (Table 5). In LQT3 CMs, compared to mexiletine, **1**, *N*-methyl-, *N*-propyl-, *N*-butyl-, *N*-ethyl methoxy-, and *N*-benzyl-substituted compounds (i.e., **43**, **44**, **45**, **46**, and **47**) were less potent at fold shortening the APD by 17, 10, 10, 5, and 5%, respectively. However, more lipophilic *N*-ethyl phenyl mexiletine (i.e., **50**) was 28% more potent at shortening the APD than mexiletine. Compared to mexiletine, the more polar *N*-acetyl phenyl-substituted compound **52** increased shortening of the APD 9%. In contrast, in normal CMs, compounds **45**–**52** did not cause detectable shortening of the APD and in some cases (i.e., compounds **43**, **45**, **46**, **49**, and **50**) caused prolongation of the APD at relatively low doses (Table 5).

Except compound **52**, of the *N*-substituted derivatives of mexiletine tested (i.e., **45**–**51**), cessation of cell beating in normal CMs was observed only at elevated doses (i.e., 133–200 μM). However, in LQT3 CMs, lipophilic compounds **46** and **50** caused cessation of cell beating at relatively low doses (i.e., 66 and 7.4 μM, respectively) (Table 5). Except compounds **43** and **50**, in normal CMs, compounds **44**–**49** either did not cause EADs or only caused EADs at elevated doses (i.e., 66 μM).

Generally, *N*-substituted mexiletines examined possessed significant potency for shortening the APD (i.e., EC_{50} for shortening), and aside from compound **52**, most compounds that provided EC_{50} values were below 2 μM in LQT3 CMs (Table 5). Based on the potency of shortening the APD by *N*-substituted derivatives of mexiletine, additional derivatives combining beneficial properties of the phenoxy ring and substituents on the amine nitrogen of phenyl mexiletine were synthesized and tested.

Region III. *N*-Substituted Analogues of Phenoxy-Substituted Phenyl Mexiletine. The effect of *N*-substitution on the pharmacological properties of phenyl mexiletine and analogues was investigated. Compared to phenyl mexiletine, most *N*-substituted-2,3-dimethyl phenoxy-substituted phenyl mexiletine compounds examined decreased fold shortening of the APD (Table 6). In LQT3 CMs, compared to phenyl mexiletine, (i.e., compound **5**), *N*-methyl, *N*-butyl, and *N*-ethyl methoxy-2,3-dimethyl phenoxy-substituted compounds (i.e., **55**, **58**, and **59**) were more potent at shortening the APD by 9, 18, and 22%, respectively. The more lipophilic *N*-ethyl methoxy 3,5-ditrifluoromethyl phenoxy-substituted phenyl mexiletine (i.e., **61**) was 28% more potent at shortening

https://doi.org/10.1021/acs.jmedchem.0c01545
J. Med. Chem. 2021, 64, 5384–5403

Table 6. Effect of *N*-Substituted Phenoxy-Substituted Phenyl Mexiletine Analogues on Cardiovascular Properties in Human iPSC-Derived Cardiomyocytes[a]

		LQT3 Cells				Normal Cells		
Number	Compd	Cessation Dose[b] (μM)	EC_{50} Shortening[c] (μM)	Fold-Shortening[d]	Maximal Shortening Dose[e] (μM)	Cessation Dose[b] (μM)	EAD Dose[f] (μM)	Fold-Prolongation[g]
5	Phenyl Mexiletine	66	< 0.8	1.174	2.5	133	-	4.0
53	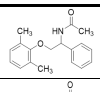	66	0.8	1.62	22	-	-	-
54	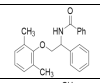	-	0.8	1.64	66	-	-	-
55	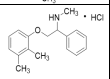	66	-	1.29	22	133	-	-
56	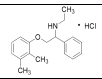	22	-	-	-	133	-	-
57	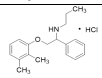	133	-	-	-	-	-	-
58	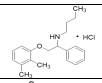	200	20.16	1.423	133	133	-	-
59	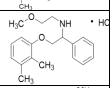	200	5.73	1.508	133	-	-	-
60	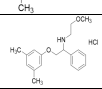	200	-	-	-	200	-	-
61	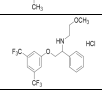	66	6.59	1.636	66	-	-	-
62	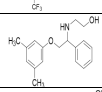	22	-	1.5	22	66	-	-
63	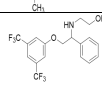	22	-	1.5	7.4	66	-	-

[a]Kinetic imaging cytometer assay results for *N*-substituted phenyl mexiletine derivatives. [b]Lowest dose that cessation of beating was observed. [c]EC_{50} for shortening the AP. [d]Ratio of AP untreated/AP treated. [e]Maximal dose that shortens the AP. [f]Dose that early after depolarization was observed. [g]EC_{50} for prolongation of the AP. The symbol "-" denotes that the indicated effect was not observed.

the APD than phenyl mexiletine. Compared to phenyl mexiletine, the somewhat more polar *N*-ethyl hydroxyl 3,5-dimethyl phenoxy-substituted phenyl mexiletine, compound **62**, increased shortening of the APD by 28%. In contrast, in normal CMs, compounds **53**−**63** did not cause detectable shortening of the APD nor did these compounds cause prolongation of the APD (Table 6).

Except compounds **62** and **63** of the *N*-substituted derivatives of phenyl mexiletine examined (i.e., **53**−**63**), cessation of cell beating in normal cardiomyocytes was observed only at elevated concentrations (i.e., 133−200 μM). However, in LQT3 CMs, somewhat polar compounds **62** and **63** and compound **56** caused cessation of cell beating at a relatively low concentration (i.e., 22 μM, respectively) (Table 6). In normal CMs, compounds **53**−**63** did not cause EADs.

Generally, *N*-substituted phenyl mexiletine analogues examined possessed significant potency for shortening the APD (i.e., EC_{50} for shortening), and aside from compound **58**, most compounds that provided EC_{50} values were below 7 μM in LQT3 CMs (Table 6). The potency of shortening the APD by *N*-substituted derivatives of phenyl mexiletine was significant and showed that *N*-substituents on phenyl mexiletine were tolerated. In general, results indicated that *N*-alkylation decreased prolongation effects and did not induce EADs. Compared to phenyl mexiletine, the *N*-methoxyethyl derivative of a number of phenyl mexiletines displayed similar shortening to the parent compound and decreased prolongation effects (Table 6). Certain *N*-substituted phenyl mexiletine analogues examined possessed significant potency for shortening the APD (i.e., EC_{50} for shortening). For example, compounds **53** and **54** afforded EC_{50} values of 0.8 μM in LQT3 CMs (Table 6). Compounds **58**, **59**, and **61** were less potent at shortening the APD (i.e., EC_{50} for shortening: 20, 5.7, and 6.6 μM, respectively).

Automated Patch Clamp Studies of Mexiletine Analogues. Automated patch clamp experiments were done to determine IC_{50}s for peak (I_{NaP}) and late sodium current (I_{NaL}) inhibition and potassium current (I_{Kr}) inhibition for selected compounds. Mexiletine and analogues were applied

https://doi.org/10.1021/acs.jmedchem.0c01545
J. Med. Chem. 2021, 64, 5384−5403

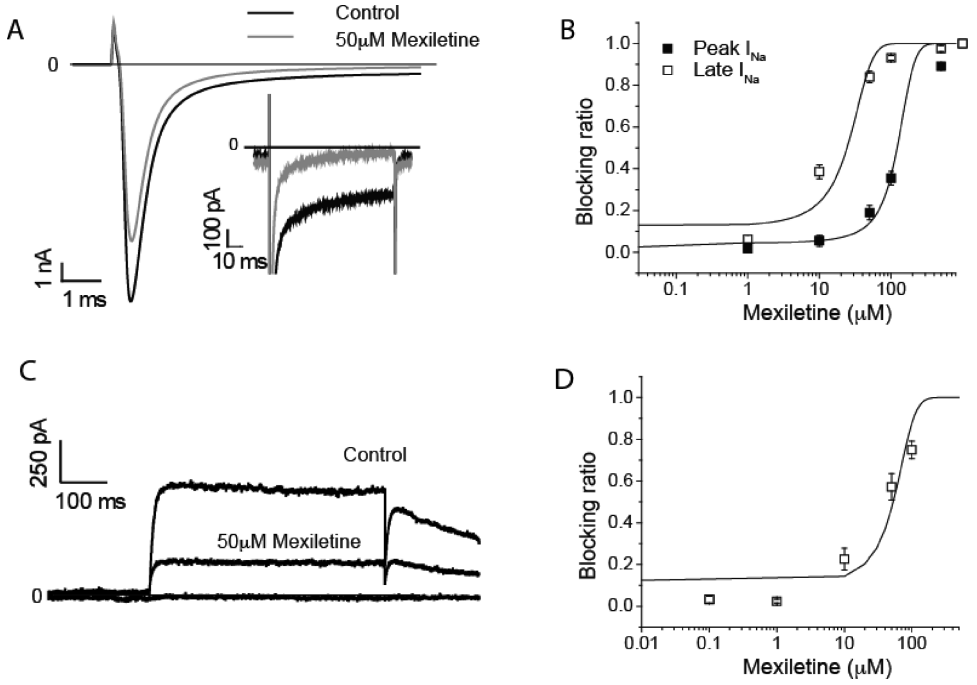

Figure 3. Traces of automated patch clamp studies. Panel (A) shows low-gain Na^+ channel signals where peak block was measured for a given concentration and high-gain (inset) traces for late current. Panel (B) shows dose−response relationships for the peak and late Na^+ current. Panels (C) and (D) show the analogous information for I_{Kr} block with current traces in panel (C) and dose−response in panel (D). Recordings were analyzed at low (I_{NaP}) and high (I_{NaL}) gains for each compound concentration.

Table 7. Effect of Mexiletine and Analogues on Automated Patch Clamp Dose−Response Data for Sodium and Potassium Channel-Transfected Cells

Compound	IC_{50} I_{NaL} (μM)	n	IC_{50} I_{NaP} (μM)	n	IC_{50} I_{Kr} (μM)	n	Selectivity[a]
1	22.5 ± 4.4[b]	4	182.8 ± 41.8	4	53.7 ± 8.0	7	2.4
2	11.4 ± 3.7	5	91.4 ± 12.7	5	27.6 ± 12.5	5	2.42
3	7.4 ± 0.4	4	130.4 ± 12.0	8	30.1 ± 5.2	7	4.1
10	19.0 ± 4.6	7	128.6 ± 12.8	6	84.0 ± 7.5	5	4.42
11	29.9 ± 5.4	6	128.2 ± 10.0	5	54.3 ± 11.1	6	1.81
15	51.8 ± 5.9	5	161.6 ± 21.0	4	98.0 ± 4.8	9	1.9
16	10.0 ± 4.9	7	76.8 ± 9.0	7	45.8 ± 11.8	6	4.6
24	17.3 ± 10.5	4	153.7 ± 8.3	5	49.3 ± 8.4	6	2.84
26	11.7 ± 0.8	5	20.6 ± 2.1	6	8.0 ± 1.3	6	0.7
27	0.643 ± 0.047	4	34.2 ± 6.7	9	22.9 ± 4.7	10	35.6
30	1.04 ± 0.34	7	41.1 ± 8.4	7	37.5 ± 14.0	4	36.1
36	0.20 ± 0.054	6	20.1 ± 4.1	9	6.2 ± 0.8	12	31
37	1.03 ± 0.06	10	20.0 ± 4.1	13	7.16 ± 1.2	5	19.4
38	1.03 ± 0.1	6	10.9 ± 0.7	10	9.2 ± 1.3	9	8.9
43	36.0 ± 3.2	5	124.1 ± 5.9	5	44.1 ± 2.2	7	1.2
59	0.747 ± 0.063	6	25.8 ± 6.6	7	27.6 ± 4.2	7	34.5
60	0.753 ± 0.094	4	38.0 ± 7.1	7	5.1 ± 0.85	9	6.8
63	1.02 ± 0.02	10	45.1 ± 9.2	10	16.8 ± 2.4	6	16.5

[a]Selectivity is defined as IC_{50} for the lesser of the ratios of I_{NaP}/I_{NaL} or I_{Kr}/I_{NaL}. [b]Data presented as mean ± standard error, n = number of replicate determinations. Sodium channel SCN5A (F1473C mutant) was transfected into HEK cells and potassium channel was transfected into CHO cells.

over a concentration range from 0.1 to 100 μM, and inhibition relative to vehicle control was determined at a steady state (~3 min) for each concentration. For I_{NaL}, data were recorded and peak channel currents were measured in response to 100 ms voltage steps to −10 mV imposed from a holding potential of −100 mV at a rate of 0.1 Hz (Figure 3, panel A). Compounds were applied to the extracellular compartment in increasing concentrations from 0 (i.e., DMSO vehicle control) to 100 μM. The ratio of IC_{50} values for inhibition of Na^+ channels was determined by normalizing measured current to control recordings for both I_{NaP} and I_{NaL} in the presence of a constant vehicle (DMSO, 0.1%). Tetradotoxin (TTX), 50 μM, was applied at the end of the experiments, so TTX currents could be subtracted from the rest of the traces to identify only sodium channels.

For I_{Kr} experiments, cells were held at −80 mV and activating pulses (500 ms) were applied at +40 mV followed by a return potential of −40 mV (0.1 Hz) whereupon deactivating tail currents were measured. Currents were recorded again over a concentration range of 0.1 to 100 μM and were normalized

https://doi.org/10.1021/acs.jmedchem.0c01545
J. Med. Chem. 2021, 64, 5384−5403

to control recordings (including 0.1% vehicle (DMSO)). The resulting peak tail current was then plotted versus test compound concentration to determine concentration−response relationships for test compounds and I_{Kr} inhibition (Figure 3, panels C and D). The selective I_{Kr} inhibitor E-4031, 5 μM, was used as a control inhibitor.

Table 7 shows automated patch clamp IC_{50} values for I_{NaL}, I_{NaP}, and I_{Kr} obtained for each of the 18 compounds examined with an $n \geq 4$ for computed IC_{50} values. Also included is a calculation for overall selectivity for inhibiting peak sodium current over late sodium current (i.e., I_{NaP}/I_{NaL}) or I_{Kr} over late sodium current (i.e., I_{Kr}/I_{NaL}). Essentially, all compounds examined were selective for late sodium current over peak sodium current and hERG. Compared to mexiletine, there were compounds that were more selective and more potent late sodium current inhibitors. Consistent with a prior report,[24] mexiletine was measured to have IC_{50} values of 22.5 ± 4.4 and 182.8 ± 41.8 μM for late and peak Na currents, respectively, and 53.7 ± 8.0 μM for I_{Kr}. Compared to mexiletine, replacement of the alpha methyl group with *tert*-butyl (i.e., **2**) or cylopropyl (i.e., **3**) had only modest changes in channel selectivity. Modification of the phenoxy ring of mexiletine (i.e., **15**, **16**, or **24**) also had modest changes on channel ratios. In contrast, alpha phenyl group modification (i.e., **30**, **33**, **39**, **40**, and **41**) afforded compounds with, in some cases, relatively great selectivity for I_{NaP} (i.e., I_{Kr}/I_{NaP} ratios of 31−36-fold). The selectivity of *N*-methyl substituted mexiletine (i.e., **43**) was no different from that of mexiletine itself. However, *N*-substitution of alpha phenyl mexiletine analogues (i.e., **59**, **60**, and **63**) in some cases showed a significant I_{Kr}/I_{NaP} selectivity (i.e., 17−35-fold). Accordingly, based on the kinetic image cytometry results and the automated patch clamp IC_{50} profiles of channel inhibition, certain compounds were advanced to further study. For selective late current block, we examined compounds in greater detail that were maximally selective over both I_{NaP} and I_{Kr} in electrophysiology experiments.

Pharmaceutical Properties of Mexiletine and Analogues. The chemical and metabolic stabilities of certain mexiletine analogues were examined in advance of *in vivo* or *ex vivo* studies. Because one of the objectives was to develop a compound that possessed lower metabolic clearance than mexiletine, the effect of varying substituents of select compounds on metabolic stability was investigated (Table 8). Racemic compounds **27**, **30**, **36**, and **59** possessed metabolic stability (in human liver microsomes + NADPH of $T_{1/2}$ > 60 min) and chemical stability ($T_{1/2}$ > 30 days, pH 7.4, phosphate buffer, 37 °C) (data not shown) as judged by HPLC analysis. At pH 3, compounds **27** and **30** had $T_{1/2}$ of >15 days and **33** and **59** had $T_{1/2}$ of >30 days. (*R*)- and (*S*)-Enantiomers of **27**, **30**, and **36** were prepared and tested for stereoselective hepatic metabolism. Time-course studies (i.e., up to 1 h incubations at 37 °C in the presence of 0.5 mM NADPH) were conducted. In the presence of human liver S-9, the (*R*)-enantiomers of **27** and **36** appeared to be more metabolically labile than their corresponding (*S*)-enantiomers. Compared to (*R*)- and (*S*)-mexiletine and (*R*)- and (*S*)-**59** and -**30** and (*S*)-**27** and (*S*)-**36** that did not have detectable metabolism in the presence of S-9, compounds (*R*)-**27** and (*R*)-**36** had $T_{1/2}$ values of 408 and 1015 min, respectively. In the presence of human liver microsomes, the (*R*)-enantiomers of **30** and **36** appeared to be more metabolically labile than their corresponding (*S*)-enantiomers. Both (*R*)- and (*S*)-mexiletine, -**27** and -**59**, did not have detectable metabolism in the presence of human liver microsomes. Highly purified human CYP3A4, 3A5, and 2D6 metabolized racemic mexiletine (46.2, 48.8, and 6.0 pmol/min/μg of protein, respectively). Highly purified CYP3A4, 3A5, and 2D6 metabolized racemic compound **30** (15.4, 42.6, and 43.6 pmol/min/μg of protein, respectively). Racemic compound **36** was detectably metabolized by highly purified CYP2D6 (6.9 pmol/min/μg of protein) but not CYP3A4 and CYP3A5. Metabolism of racemic **27** and **59** in the presence of highly purified CYP was not conducted.

***In Vivo* Studies of Mexiletine and Analogues.** Based on *in vitro* metabolism data, pharmacokinetics (PK) studies of mexiletine, racemic **30**, and its enantiomers were examined (Table 9). Animals were administered by intravenous (5 mg/kg) or oral (25 mg/kg) routes to obtain bioavailability (*F*) data. Compared to PK parameters of mexiletine, racemic **30**, (*R*)-**30**, and (*S*)-**30** afforded superior oral administration PK properties. This included acceptable half-lives, greater peak onset (C_{max}), and greater bioavailability (*F*). Compared to mexiletine (*F* = 37%), (*R*)-**30** (100%) possessed superior oral PK properties. Bioavailability values for (*S*)-**30** and rac-**30** were 42 and 38%, respectively.

Behavioral Studies of Mexiletine and Analogues in Mice. Previously, it was reported that mexiletine has an LD_{50} of 115 mg/kg in mice.[25] In our hands, significant behavioral effects (i.e., seizures and deaths) were observed for mexiletine at 100 and 200 mg/kg (i.p.). In contrast, we observed that synthetic phenyl mexiletine analogues examined possessed LD_{50} > 200 mg/kg (i.p.) in mice. Administration of 200 mg/kg (i.p.) of (*R*)- or (*S*)-enantiomers of **27**, **30**, **36**, or **59** did not show any lethality. Thus, the LD_{50} was >200 mg/kg for the phenyl mexiletine compounds examined.

Among the adverse reactions in rodents[26] and human patients[27] administered (*R*)-mexiletine are nausea and seizures. We examined the behavioral properties of enantiomerically pure **27**, **30**, **36**, or **59** and compared them to (*R*)- or (*S*)-mexiletine at 100 mg/kg (Table 10). The phenyl mexiletine enantiomers (i.e., enantiomers of **27**, **30**, **36**, or **59**) were relatively well-tolerated *in vivo* (100 mg/kg, i.p.). For (*R*)-mexiletine, administration of 100 mg/kg produced immobilization, seizures, and death. (*S*)-Mexiletine (100 mg/kg) produced lethargy and immobilization, but severe seizures were not observed. In contrast, mice treated with enantiomer (*R*)-**30**, **36**, or **59** (100 mg/kg) showed no apparent behavioral effects although (*R*)-**27** showed some immobilization effects. Lethargy and other central nervous system effects were

Table 8. Metabolic Stability of Mexiletine and Analogues with Human Liver Preparations

	$T_{1/2}$ (min)	
Compound number	Human liver S-9	Human liver microsomes
(*R*)-mexiletine	>95% after 1 h	>95% after 1 h
(*S*)-mexiletine	>95% after 1 h	>95% after 1 h
(*R*)-**27**	408 min	365 min
(*S*)-**27**	>95% after 1 h	136 min
(*R*)-**30**	>95% after 1 h	>95% after 1 h
(*S*)-**30**	>95% after 1 h	>95% after 1 h
(*R*)-**36**	1015 min	406 min
(*S*)-**36**	>95% after 1 h	>95% after 1 h
(*R*)-**59**	>95% after 1 h	>95% after 1 h
(*S*)-**59**	1040 min	>95% after 1 h

https://doi.org/10.1021/acs.jmedchem.0c01545
J. Med. Chem. 2021, 64, 5384−5403

Table 9. Effect of Mexiletine and Analogues on Pharmacokinetic Parameters in Rats[a]

Compound	Route of administration	T_{max} (h)	C_{max} (mg/mL)	AUC (h × ng/mL)	$T_{1/2}$ (h)
Mexiletine	i.v.	0.17	289 ± 39	447 ± 47	10.6
	oral	1.0	167 ± 41	839 ± 456	11
	F = 37%				
(Rac)-**30**	i.v.	0.17	250 ± 16	544 ± 27	3.2
	oral	1.5	226 ± 15	1008 ± 227	6.5
	F = 38%				
(***R***)-**30**	i.v.	0.18	249 ± 2	280 ± 59	1.2
	oral	1.5	258 ± 2	1556 ± 19	5.3
	F = 100%				
(***S***)-**30**	i.v.	0.17	219 ± 15	407 ± 34	3.8
	oral	1.5	226 ± 15	1008 ± 227	6.5
	F = 42%				

[a]Two-four male rats for each route of administration.

Table 10. Effect of Mexiletine and Analogues on Behavior in Mice

Compound	Behavioral effect ((*R*)-enantiomer)[a]	Behavioral effect ((*S*)-enantiomer)[a]
Mexiletine	1 seizure, 1 death, 2 immobilized	4/4 immobilized
27	4/4 immobilized	3/4 immobilized
30	No detectable effect	2/4 slightly lethargic
36	No detectable effect	2/4 lethargic
59	No detectable effect	2/4 shaking

[a]Four mice were administered 100 mg/kg compound, i.p. Behavioral effects were monitored for 30 min. Lethality was measured after 24 h.

observed for (*S*)-**27**, **30**, **36**, or **59** at 100 mg/kg. Thus, behavioral effects for phenyl mexiletines **30**, **36**, or **59** were stereoselective (i.e., behavioral toxicity was (*S*)- > (*R*)-enantiomer). In conclusion, compared to mexiletine, it was apparent that (*R*)-enantiomers of compounds **30**, **36**, and **59** examined showed considerably less toxicity (i.e., seizures and death) than that observed for mexiletine enantiomers.

***Ex Vivo* Studies of (*R*)-30 with Rat Heart Preparations.** As an adjunct to LQT3 *in vitro* studies, we conducted *ex vivo* studies of (*R*)-**30** in aged rats. In this model, conduction velocity (CV), action potential duration (APD), and responsiveness to drugs were measured in perfused *ex-vivo* rat heart preparations (Figure 4a). *Ex vivo* heart preparations can be used to study the effect of compounds to decrease arrhythmias because CV and APD are preserved in buffer-perfused rat hearts for up to 2 days. We chose a rat heart model to test the effects of (*R*)-**30** *ex vivo* because (*R*)-**30** is potent and stereoselective, not extensively metabolized, has good bioavailability and solubility (8−10 mg/mL water), and no apparent toxicity up to 200 mg/kg (i.p.). In this perfused *ex-vivo* rat heart model, the continuous presence (perfusion) of H_2O_2 (0.1 mM) produced EADs and ectopic ventricular beats 6 min after exposure that degenerated to ventricular tachycardia (VT) and ventricular fibrillation (VF) after 12 min (Figure 4b). Left untreated, these perfused hearts generally die within 45 min. Using this preparation, complete resolution of all forms of arrhythmias to normal sinus rhythm was observed 30−40 min after administration of compound (*R*)-**30** (10 μM) in the continuous presence of H_2O_2 (0.1 mM) (Figure 4c). This shows that administration of (*R*)-**30** to a heart suffering from severe arrhythmias potently reverses VT and VF and corrects EADs in a very short time. This may be clinically relevant. The effect of (*R*)-**30** is similar to or more potent than the effect of ranolazine (10 μM) in the same *ex vivo* model[28] or GS-967 or roscovitine in related *ex vivo* models.[28] The conclusion is that (*R*)-**30** is more efficacious than the currently used standard of care.

CONCLUSIONS

Patient-derived iPSC CMs combined with dynamic medicinal chemistry were used to re-engineer mexiletine. Replacement of metabolically labile mexiletine substituents with more metabolically resilient groups (e.g., $-CF_3$ for $-CH_3$) improved the pharmaceutical and pharmacological properties of the molecule. The combination of drug design in a dish and disease in a dish approaches was shown to be useful to identify more potent, selective, less toxic analogues of mexiletine that may hold clinical relevance. In addition, compounds such as relatively long-lived (*R*)-**30** possessing later T_{max} and greater oral C_{max} and AUC with good *ex vivo* efficacy showed that major shortcomings of mexiletine (the need for multiple and repeated administration and toxicity) have potentially been overcome.

METHODS

General. Reagents, starting materials, and solvents were purchased in the highest purity available from commercial suppliers and used as received. Mexiletine, (*R*)-mexiletine, and (*S*)-mexiletine were purchased from Toronto Research (Toronto, CA). Hydrochloride salts were prepared by dissolution of the appropriate compound in a minimum amount of dichloromethane and addition of excess 2 M HCl in ether. The solvent was evaporated, and hydrochlorides were used directly for evaluation. Phosphate-buffered saline (PBS) and SYBR Green used in cell proliferation assays were purchased from Life Technologies (Carlsbad, CA). Fluorescence was determined using a Tecan SPECTRAFluor Plus plate reader (Tecan, San Jose, CA). Luminescence was recorded on a Wallac Victor plate reader (PerkinElmer Inc., Waltham, MA).

Chemistry Experimental Section. Experiments were carried out under an inert atmosphere when oxygen- or moisture-sensitive reagents or intermediates were employed. Commercial solvents and reagents were used without further purification. Microwave reactions were conducted using a Biotage Initiator microwave synthesizer (Biotage, Uppsala, Sweden). Reaction products were purified, when necessary, using an Isco Combiflash R_f flash chromatography system (Teledyne-Isco, Lincoln, NE) with the solvent systems indicated. Nuclear magnetic resonance (NMR) data were recorded on a Varian Mercury 300 MHz spectrometer (Agilent, Santa Clara, CA) unless specified or in a Bruker 500 MHz instrument at NuMega Resonance Laboratories (San Diego, CA) in the indicated solvents. Chemical shifts for nuclear magnetic resonance (NMR) data were expressed in

https://doi.org/10.1021/acs.jmedchem.0c01545
J. Med. Chem. 2021, 64, 5384−5403

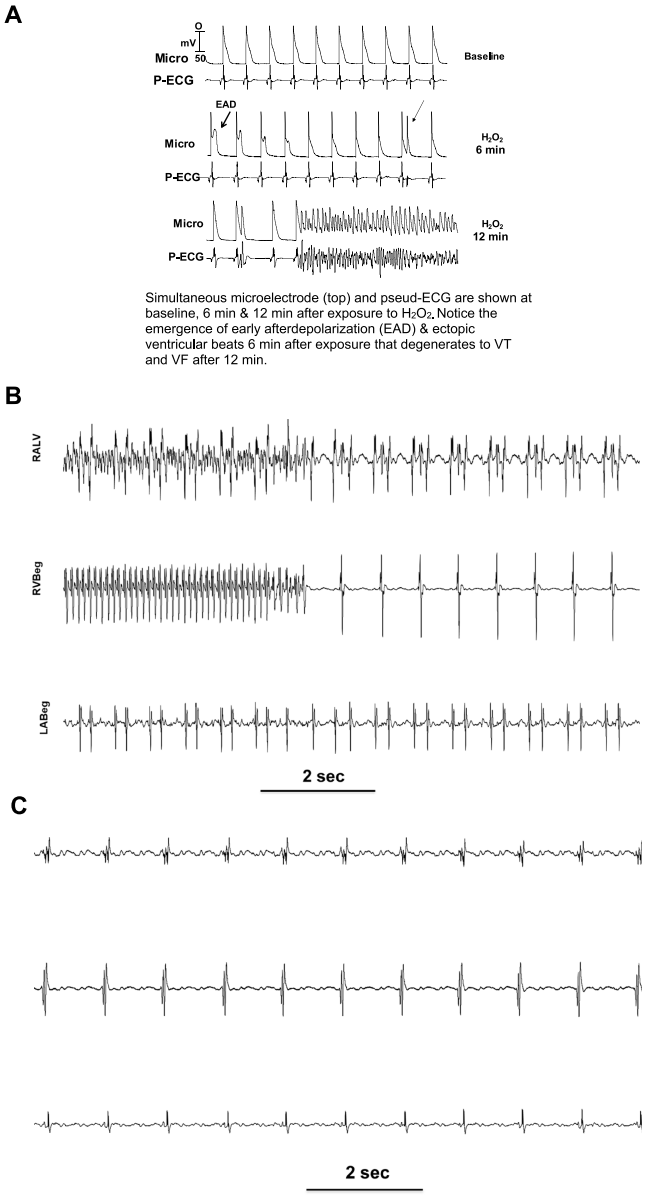

Figure 4. (A) Initiation of early after depolarizations-mediated ectopic ventricular beats and ventricular fibrillation in an isolated perfused aged rat heart exposed to hydrogen peroxide. (B) Representative example of administration of compound (*R*)-**30** (10 μM) after 20 min to an aged rat heart perfused with H_2O_2 (0.1 mM). Note that compound (*R*)-**30** suppressed ventricular fibrillation (VF) by conversion to monomorphic ventricular tachycardia (VT) and then to sinus rhythm. (C) In the aged rat heart (treated as in Figure 4A) with continued perfusion of H_2O_2 (0.1 mM) and treatment with compound (*R*)-**30** (10 μM) after 40 min, the heart continued to show sustained sinus rhythm. Complete resolution of all forms of arrhythmias to normal sinus rhythm 30−40 min after perfusion of compound (*R*)-**30** (10 μM) was observed in an isolated perfused aged heart in the presence of hydrogen peroxide.

parts per million (ppm, δ) referenced to residual peaks from deuterated solvents. Mass spectrometry (MS) data were reported from liquid chromatography−mass spectrometry (LCMS) instrumentation. Electrospray ionization (ESI) mass spectral data were obtained using an Agilent 1100 LC/MS (Agilent, Santa Clara, CA). Final test compounds were pure based on LCMS analysis using UV−vis detection at 275 and 220 nM. Mexiletine and analogue compound purities were determined by high-performance liquid chromatography (HPLC), and all final test compounds were of >95% purity. Final compounds were assessed for purity by HPLC via the following conditions: column: Waters Atlantis dC18 4.6 × 50, 5 um; mobile phase A: 0.05% TFA in water (v/v); mobile phase B: 0.05% TFA in acetonitrile (v/v); gradient: 95.0% water/5.0% acetonitrile linear to 5% water/95% acetonitrile in 4.0 min, hold at 5% water/95% acetonitrile to 5.0 min; flow: 2 mL/min. Samples analyzed for ESI-TOF high-accuracy mass spectroscopy were sent for analysis at the mass spectroscopy service at The Scripps Research Institute, San Diego, CA.

Chiral compounds were analyzed using a Hitachi-7100 HPLC system equipped with a Phenomenex Lux 5 μm Cellulose-1 150 × 4.6 mm column. Detection was achieved with a Hitachi-7400 UV detector with monitoring at 220 nm. Compounds were eluted with a mixture of 70:20:5 hexanes/isopropanol/acetonitrile containing 0.02% perchloric acid with a flow rate of 0.5 mL/min.

Syntheses of Amines via Reduction of *O*-Benzyloximes. *1-(2,6-Dimethylphenoxy)-3,3-dimethylbutan-2-amine (**2**). Step 1: 1-(2,6-Dimethylphenoxy)-3,3-dimethylbutan-2-one.* To a mixture of 1-bromo-3,3-dimethylbutan-2-one (0.75 mL, 5.6 mmol) and 2,6-dimethylphenol (1.02 g, 8.3 mmol) in DMF (5 mL) was added 1.1 g (8.3 mmol) of potassium carbonate. After stirring at 21 °C for 16 h water was added and extracted with diethyl ether. The organic phase was washed (water, 2 M sodium hydroxide, brine), dried over magnesium sulfate, and concentrated under reduced pressure. The residue was purified by flash chromatography on silica gel using an ethyl acetate/hexane gradient. The target ketone was obtained (0.49 g) in 40% yield. ^{1}H NMR (300 MHz, $CDCl_3$): 7.00−7.02 (m, 2H), 6.93−6.96 (m, 1H), 4.64 (s, 2H), 2.26 (s, 6H), 1.22 (s, 9H). MS: 221.0 (MH^+).

Step 2: (E/Z)-1-(2,6-Dimethylphenoxy)-3,3-dimethylbutan-2-one O-Benzyl Oxime. To a flask containing 400 mg (1.8 mmol) of 1-(2,6-dimethylphenoxy)-3,3-dimethylbutan-2-one in 8 mL of ethanol were added *O*-benzylhydroxylamine hydrochloride (879 mg, 5.5 mmol) and pyridine (0.882 mL, 10.9 mmol) and stirred at 21 °C for 16 h, diluted with water, and extracted with diethyl ether. The organic phase was washed (water, brine), dried over sodium sulfate, and concentrated. Chromatography on silica gel using a gradient of ethyl acetate in hexane was conducted to yield 365 mg (62%) of the product as a colorless oil. ^{1}H NMR ($CDCl_3$): 1.31 (s, 9H), 2.26 (s, 6H), 4.59 (s, 2H), 5.08 (s, 2H), 6.87−6.92 (m, 1H), 6.96−6.98 (m, 2H), 7.28−7.31 (m, 5H). MS: 326.0 (MH^+).

*Step 3: 1-(2,6-Dimethylphenoxy)-3,3-dimethylbutan-2-amine (**2**).* To a flask containing 100 mg (0.31 mmol) of the above *O*-benzyl oxime in 1 mL of THF was added 1.2 mL (1.2 mmol) of a 1 M solution of borane in THF and heated at 50 °C for 16 h. The mixture was allowed to cool to room temperature and carefully stopped by addition of 6 M aqueous HCl. After about 10 min, the mixture was taken to pH > 10 by addition of an excess of 6 M aqueous sodium hydroxide and extracted with ethyl acetate. The organic phase was washed (water, brine), dried (sodium sulfate), and concentrated. Chromatographic purification using 5% methanol in dichloromethane afforded the target product. ^{1}H NMR ($CDCl_3$): 1.03 (s, 9H), 2.31 (s, 6H), 3.12−3.16 (m, 1H), 3.75−3.87 (m, 2H), 6.89−6.94 (m, 1H), 6.96−7.02 (m, 2H) MS: 222.0 (MH^+).

The following compounds were prepared using similar sequences with the appropriate starting materials:

*1-Cyclopropyl-2-(2,6-dimethylphenoxy)ethanamine (**3**).* ^{1}H NMR ($CDCl_3$): 7.03−6.90 (m, 3H), 3.90−3.77 (AB of ABX, J_{AB} = 9.0 Hz, 2H), 2.41 (m, 1H, overlapping with neighboring peak), 2.32 (s, 6H), 0.96 (m, 1H), 0.57 (m, 2H), 0.32 (m, 2H) ppm. MS: 206.2 (MH^+). R_f = 0.17 (10% methanol in dichloromethane, silica gel).

*1-Cyclohexyl-2-(2,6-dimethylphenoxy)ethan-1-amine (**4**).* ^{1}H NMR (300 MHz, methanol-d_4) δ 1.15−1.39 (m, 5H), 1.63−2.05 (m, 6H), 2.30 (s, 6H), 3.41 (td, J = 3.7, 7.2 Hz, 1H), 3.66 (s, 1H), 3.86−4.05 (m, 1H), 6.87−7.07 (m, 2H). MS: 248.2 (MH^+).

*2-(2,6-Dimethylphenoxy)-1-phenylethanamine (**5**).* ^{1}H NMR ($CDCl_3$): 7.43−7.46 (m, 2H), 7.27−7.37 (m, 3H), 6.97−6.99 (m, 2H), 6.87−6.92 (m, 1H), 4.46 (dd, J = 4.7 and 8.0 Hz, 1H), 3.79−3.89 (m, 2H), 2.25 (s, 6H). MS: 242.2 (MH^+).

https://doi.org/10.1021/acs.jmedchem.0c01545
J. Med. Chem. 2021, 64, 5384−5403

*2-(2,6-Dimethylphenoxy)-1-p-tolylethanamine (**6**).* ^{1}H NMR ($CDCl_3$): 2.29 (s, 6H), 2.36 (s, 3H), 3.78−3.87 (m, 2H), 4.43 (dd, J = 4.1 and 8.0 Hz, 1H), 6.88−6.93 (m, 1H), 6.98−7.01 (m, 2H), 7.17 (d, J = 8.0 Hz, 2H), 7.33 (d, J = 8.0 Hz, 2H). MS: 256.2 (MH^+).

*2-(2,6-Dimethylphenoxy)-1-(4-(trifluoromethyl)phenyl)-ethanamine (**7**).* ^{1}H NMR ($CDCl_3$): 2.23 (s, 6H), 3.78−3.88 (m, 2H), 4.51 (dd, J = 4.4 and 4.4 Hz, 1H), 6.88−6.93 (m, 1H), 6.97−7.00 (m, 2H), 7.56−7.72 (m, 4H). MS: 309.2 (MH^+).

*2-(2,6-Dimethylphenoxy)-l-(4-methoxyphenyl)ethanamine (**8**).* ^{1}H NMR ($CDCl_3$): 7.36 (s, J = 8.8 Hz, 2H), 6.97−6.99 (m, 2H), 6.85−6.92 (m, 3H), 4.39−4.43 (m, 1H), 3.80 (s, 3H), 3.79−3.82 (m, 2H), 2.26 (s, 6H). MS: 272.1 (MH^+).

*2-(2,6-Dimethylphenoxy)-1-(naphthalen-2-yl)ethan-1-amine (**9**).* ^{1}H NMR (300 MHz, DMSO-d_6) δ 8.95 (s, 3H), 8.15 (s, 1H), 7.97 (m, 3H), 7.77 (d, J = 8.5 Hz, 1H), 7.57 (dd, J = 5.7, 3.8 Hz, 2H), 7.01−6.87 (m, 3H), 4.90 (s, 1H), 4.38−4.00 (m, 2H), 2.10 (s, 6H). MS: 292.1 (MH^+). R_f = 0.52 (5% methanol in dichloromethane on silica).

*1-Cyclopropyl-2-(2,6-dimethylphenoxy)ethan-1-amine (**12**).* ^{1}H NMR ($CDCl_3$): 7.03−6.90 (m, 3H,), 3.90−3.77 (AB of ABX, J_{AB} = 9.0 Hz, 2H), 2.41 (m, 1H, overlapping with neighboring peak), 2.32 (s, 6H), 0.96 (m, 1H), 0.57 (m, 2H), 0.32 (m, 2H). MS: 206.2 (MH^+).

*1-Cyclopropyl-2-(2,4-dimethylphenoxy)ethan-1-amine (**13**).* ^{1}H NMR (300 MHz, CD_3OD) 6.90−7.00 (m, 2H), 6.77−6.86 (m, 1H), 4.06−4.28 (m, 2H), 2.84 (ddd, J = 3.4, 6.3, 10.0 Hz, 1H), 2.24 (broad s, 6H), 1.11 (m, 1H), 0.78 (ddd, J = 2.0, 3.8, 8.0 Hz, 2H), 0.45−0.63 (m, 2H). MS: 206.2 (MH^+).

*1-Cyclopropyl-2-(3,4-dimethylphenoxy)ethan-1-amine (**14**).* ^{1}H NMR (300 MHz, CD_3OD) 7.03 (d, J = 8.2 Hz, 1H), 6.80 (d, J = 2.8 Hz, 1H), 6.72 (dd, J = 2.7, 8.2 Hz, 1H), 4.23 (dd, J = 3.5, 10.3 Hz, 1H), 4.09 (dd, J = 7.0, 10.3 Hz, 1H), 2.79 (ddd, J = 3.5, 7.0, 10.4 Hz, 1H), 2.2.4 (s, 3H), 2.20 (s, 3H), 1.07−1.24 (m, 1H), 0.70−0.82 (m, 2H), 0.54 (qd, J = 4.9, 10.2 Hz, 2H). MS: 206.2 (MH^+).

*1-Cyclopropyl-2-(3,5-dimethylphenoxy)-N-(2-methoxyethyl)-ethan-1-amine (**15**).* ^{1}H NMR (300 MHz, CD_3OD) 6.58 (s, 1H), 6.54 (s, 2H), 4.05−4.16 (m, 1H), 4.05−4.16 (m, 1H), 3.44−3.63 (m, 2H), 3.37 (s, 3H), 2.95−3.16 (m, 1H), 2.73−2.95 (m, 1H), 2.10−2.22 (m, 1H), 0.45−0.61 (m, 1H), 0.32−0.47 (m, 2H), 0.14−0.32 (m, 2H). MS: 264.2 (MH^+).

*1-Cyclopropyl-2-(3,5-dimethylphenoxy)ethan-1-amine (**16**).* ^{1}H NMR (300 MHz, $CDCl_3$): 8.67 (br. s., 3H), 6.68 (s, 2H), 6.58 (s, 1H), 3.85−4.39 (m, 2H), 2.26 (s, 6H), 2.16−2.39 (m, 1H), 1.82−2.10 (m, 1H), 0.93−1.30 (m, 2H), 0.52 (m, 2H). MS: 206.2 (MH^+).

*1-(2-Methylphenoxy)propan-2-amine (**17**).* ^{1}H NMR (300 MHz, $CDCl_3$): 7.16 (m, 2H), 6.87 (td, J = 7.5, 1.1 Hz, 1H), 6.82 (m, 1H), 3.93−3.70 (AB of ABX, J_{AB} = 8.8 Hz, 2H), 3.41 (m, 1H), 2.27 (s, 3H), 1.23 (d, J = 6.6 Hz, 1H). MS: 166.1 (MH^+). R_f = 0.20 (15% methanol in dichloromethane on silica gel).

*1-(2-Ethylphenoxy)propan-2-amine (**18**).* ^{1}H NMR (300 MHz, $CDCl_3$): 7.16 (m, 2H), 6.92 (td, J = 7.4, 1.1 Hz, 1H), 6.82 (dd, J = 8.8, 0.9 Hz, 1H), 3.92−3.71 (AB of ABX, J_{AB} = 9.0 Hz, 2H), 3.41 (m, 1H,), 2.69 (q, J = 7.5 Hz, 2H), 1.24 (t, J = 7.5 Hz, 3H), 1.23 (d, J = 6.6 Hz, 1H). MS: 180.1 (MH^+). R_f = 0.22 (15% methanol in dichloromethane on silica gel).

*1-(2-Propylphenoxy)propan-2-amine (**19**).* ^{1}H NMR (300 MHz, $CDCl_3$): 7.15 (m, 2H), 6.89 (td, J = 7.4, 1.4 Hz, 1H), 6.82 (m, 1H), 3.92−3.70 (AB of ABX, J_{AB} = 8.8 Hz, 2H), 3.41 (m, 1H), 2.64 (t, J = 7.5 Hz, 2H), 1.64 (m, 2H), 1.23 (d, J = 6.6 Hz, 1H), 0.98 (t, J = 7.1 Hz, 3H). MS: 194.1 (MH^+). R_f = 0.24 (15% methanol in dichloromethane on silica gel).

*1-(2-(Trifluoromethyl)phenoxy)propan-2-amine (**20**).* ^{1}H NMR (300 MHz, $CDCl_3$): 7.57 (dd, J = 7.7, 1.3 Hz, 1H), 7.48 (m, 1H), 7.00 (m, 2H), 4.03−3.76 (AB of ABX, J_{AB} = 8.5 Hz, 2H), 3.44 (m, 1H), 1.23 (d, J = 6.6 Hz, 1H) ppm. MS: 220.0 (MH^+). R_f = 0.16 (15% methanol in dichloromethane on silica gel).

*1-(2-Methoxyphenoxy)propan-2-amine (**21**).* 1H NMR (300 MHz, $CDCl_3$): 6.96−6.88 (m, 4H), 3.98−3.70 (AB of ABX, J_{AB} = 9.4 Hz, 2H), 3.88 (s, 3H), 3.41 (m, 1H), 1.20 (d, J = 6.6 Hz, 1H). MS: 183.1 (MH^+). R_f = 0.29 (15% methanol in dichloromethane on silica gel).

*1-(m-Tolyloxy)propan-2-amine (**22**).* ^{1}H NMR (500 MHz, CD_3OD) 7.11−7.23 (m, 1H), 6.69−6.90 (m, 3H), 4.09−4.23 (m, 1H), 3.91−4.04 (m, 1H), 3.66−3.76 (m, 1H), 2.32 (s, 3H), 1.41 (d, = 7.1 Hz, 3H). MS: 166.1 (MH^+).

*1-(3-(Trifluoromethyl)phenoxy)propan-2-amine (**23**).* ^{1}H NMR (500 MHz, CD_3OD) 6.90−6.95 (m, 1H), 7.15−7.30 (m, 3H), 4.31 (d, J = 3.3 Hz, 1H), 4.23 (d, J = 6.6 Hz, 1H), 2.77−2.98 (m, 1H), 2.28 (s, 6H), 1.12−1.27 (m, 1H), 0.80−0.93 (m, 1H), 0.71−0.81 (m, 1H), 0.56−0.70 (m, 1H), 0.43−0.52 (m, 1H). MS: 220.1 (MH^+).

*1-(3,5-Dimethylphenoxy)propan-2-amine (**24**).* ^{1}H NMR (500 MHz, CD_3OD) 6.67 (none, 1H), 6.65 (s, 2H), 4.31 (d, J = 3.29 Hz, 1H), 4.23 (d, J = 6.57 Hz, 1H), 2.77−2.98 (m, 1H), 2.28 (s, 6H), 1.12−1.27 (m, 1H), 0.80−0.93 (m, 1H), 0.71−0.81 (m, 1H), 0.56−0.70 (m, 1H), 0.43−0.52 (m, 1H). MS: 180.0 (MH^+).

*1-(3,5-Bis(trifluoromethyl)phenoxy)propan-2-amine (**25**).* ^{1}H NMR (500 MHz, CD_3OD) 7.63−7.44 (m, 1H), 7.04−7.26 (m, 1H), 6.72−6.92 (m, 1H), 4.65−4.80 (m, 1H), 4.32−4.41 (m, 1H), 4.25−4.33 (m, 1H), 2.32 (s, 3H). MS: 288.1 (MH^+).

*2-(2,4-Dimethylphenoxy)-1-phenylethan-1-amine (**26**).* ^{1}H NMR (500 MHz, CD_3OD) 7.41−7.69 (m, 5H), 6.90−7.01 (m, 2H), 6.77−6.84 (m, 1H), 4.75−4.82 (m, 1H), 4.26−4.34 (m, 2H), 2.23 (s, 3H), 2.22 (s, 2H). MS: 242.1 (MH^+).

*1-Phenyl-2-(o-tolyloxy)ethanamine (**27**).* ^{1}H NMR (300 MHz, $CDCl_3$): 7.44−7.47 (m, 1H), 7.29−7.37 (m, 4H), 7.08−7.13 (m, 2H), 6.83−6.88 (m, 1H), 6.75−6.78 (m, 1H), 4.45−4.49 (m, 1H), 4.13 (dd, J = 4.1 and 9.1 Hz, 1H), 3.98−4.05 (m, 1H), 2.88 (bs, 2H), 2.24 (s, 3H). MS: 228.0 (MH^+). ^{13}C NMR (125 MHz, CD_3OD): 157.14, 135.27, 130.99, 130.55, 128.88, 128.23, 123.04, 115.62, 71.35, 55.81, 28.86. Calcd m/z for $[C_{15}H_{17}NO + H]^+$: 228.1383. Observed: 228.1387. MS: 228.0 (MH^+).

*2-(2-Ethylphenoxy)-1-phenylethan-1-amine (**28**).* ^{1}H NMR (300 MHz, $CDCl_3$): 7.44−7.47 (m, 1H), 7.29−7.38 (m, 4H), 7.08−7.15 (m, 2H), 6.86−6.91 (m, 1H), 6.77−6.80 (m, 1H), 4.45−4.49 (m, 1H), 4.12 (dd, J = 4.1 and 9.1 Hz, 1H), 3.99−4.05 (m, 1H), 2.65 (q, J = 7.4 Hz, 2H), 2.52 (bs, 2H), 1.18 (t, J = 7.4 Hz, 3H). MS: 242.0 (MH^+).

*1-Phenyl-2-(2-propylphenoxy)ethanamine (**29**).* ^{1}H NMR (300 MHz, $CDCl_3$): 7.44−7.47 (m, 1H), 7.29−7.38 (m, 4H), 7.08−7.14 (m, 2H), 6.84−6.90 (m, 1H), 6.77−6.80 (m, 1H), 4.44−4.48 (m, 1H), 4.11 (dd, J = 4.4 and 9.1 Hz, 1H), 3.98−4.04 (m, 1H), 2.56−2.61 (m, 2H), 2.36 (bs, 2H), 1.57 (sextet, J = 7.4 Hz, 2H), 0.95 (t, J = 7.4 Hz, 3H). MS: 256.0 (MH^+).

*1-Phenyl-2-(2-(trifluoromethyl)phenoxy)ethanamine (**30**).* ^{1}H NMR (300 MHz, $CDCl_3$): 7.54−7.58 (m, 1H), 7.44−7.49 (m, 2H), 7.29−7.42 (m, 4H), 6.98−7.03 (m, 1H), 6.91−6.94 (m, 1H), 4.48−4.58 (m, 1H), 4.19−4.27 (m, 1H), 4.02−4.11 (m, 1H), 2.38 (bs, 2H). MS: 282.0 (MH^+). ^{13}C NMR (125 MHz, CD_3OD): 157.50, 135.56, 132.08, 130.88, 130.54, 128.75, 128.25, 122.97, 113.09, 70.40, 56.11. Calcd m/z for $[C_{15}H_{14}F_3NO + H]^+$: 282.1100. Observed: 282.1089.

*2-(2-Methoxyphenoxy)-1-phenylethanamine (**31**).* ^{1}H NMR (300 MHz, $CDCl_3$): 7.47−7.50 (m, 1H), 7.30−7.39 (m, 4H), 6.86−6.98 (m, 4H), 4.48−4.52 (m, 1H), 4.15−4.20 (m, 1H), 4.05−4.11 (m, 1H), 3.79 (m, 3H), 2.68 (bs, 2H).). MS: 244.0 (MH^+).

*1-Phenyl-2-(2-(trifluoromethoxy)phenoxy)ethan-1-amine (**32**).* ^{1}H NMR (300 MHz, $CDCl_3$): 7.44−7.58 (m, 2H), 7.31−7.43 (m, 3H), 7.14−7.30 (m, 2H), 6.84−7.03 (m, 2H), 4.51 (dd, J = 3.58, 8.53 Hz, 1H), 4.15 (dd, J = 3.58, 8.80 Hz, 1H), 3.91−4.07 (m, 1H) for the free base amine. ^{1}H NMR (300 MHz, CD_3OD) d 7.41−7.63 (m, 5H), 7.26−7.39 (m, 2H), 7.17−7.25 (m, 1H), 7.00−7.13 (m, 1H), 4.80 (dd, J = 4.95, 7.15 Hz, 1H), 4.34−4.53 (m, 2H) for the hydrochloride salt. MS: 298.0 (MH^+). R_f = 0.5 (5% methanol in dichloromethane on silica gel).

*1-Phenyl-2-(2-(2,2,2-trifluoroethoxy)phenoxy)ethan-1-amine (**33**).* ^{1}H NMR ($CDCl_3$): 7.25−7.59 (m, 5H), 6.81−7.13 (m, 4H), 4.48 (d, J = 4.40 Hz, 1H), 4.29 (qd, J = 2.06, 8.39 Hz, 2H), 4.20 (td, J = 3.44, 4.75 Hz, 1H), 3.99−4.14 (m, 1H) for the amine free base. ^{1}H NMR (300 MHz, DMSO-d_6) δ 8.57 (br. s., 3H), 7.63−7.53 (m, 2H),

https://doi.org/10.1021/acs.jmedchem.0c01545
J. Med. Chem. 2021, 64, 5384−5403

7.39−7.52 (m, 2H), 7.06−7.24 (m, 3H), 6.91−7.06 (m, 2H), 4.76 (m, 1H), 4.53−4.70 (m, 2H), 4.23−4.36 (m, 2H) for the hydrochloride. MS: 311.0 (MH^+). R_f for the free base = 0.5 (5% methanol in dichloromethane on silica gel).

*1-Phenyl-2-(m-tolyloxy)ethan-1-amine (**34**).* ^{1}H NMR (500 MHz, CD_3OD): δ 7.63−7.44 (m, 1H), 7.04−7.26 (m, 1H), 6.72−6.92 (m, 1H), 4.65−4.80 (m, 1H), 4.32−4.41 (m, 1H), 4.25−4.33 (m, 1H), 2.32 (s, 3H). MS: 228.0 (MH^+).

*1-Phenyl-2-(3-(trifluoromethyl)phenoxy)ethan-1-amine (**35**).* ^{1}H NMR ($CDCl_3$): 7.27−7.49 (m, 8H), 4.48 (dd, J = 3.8, 8.6 Hz, 1H), 4.15 (dd, J = 3.8, 8.7 Hz, 1H), 4.02 (t, J = 8.7 Hz, 1H). MS: 282.0 (MH^+).

*2-(3,5-Dimethylphenoxy)-1-phenylethanamine Hydrochloride (**36**).* ^{1}H NMR (300 MHz, CD_3OD): δ 7.56−7.46 (m, 5H), 6.64 (s, 3H), 4.74 (dd, J = 8.3, 4.4 Hz, 1H), 4.35−4.24 (AB of ABX, J_{AB} = 10.5 Hz, 2H), 2.27 (s, 6H). MS: 242.0 (MH^+). ^{13}C NMR (125 MHz, CD_3OD): 159.47, 140.71, 135.41, 130.86, 130.54, 128.75, 124.65, 113.61, 69.94, 56.07, 21.07. MS: 242.0 (MH^+). Calcd m/z for $[C_{16}H_{19}NO + H]^+$: 242.1540. Observed: 242.1542.

*2-(3,5-Bis(trifluoromethyl)phenoxy)-1-phenylethan-1-amine (**37**).* ^{1}H NMR (300 MHz, $CDCl_3$): 7.27−7.49 (m, 8H), 4.48 (dd, J = 3.8, 8.6 Hz, 1H), 4.15 (dd, J = 3.8, 8.7 Hz, 1H), 4.02 (t, J = 8.7 Hz, 1H). MS: 350.0 (MH^+).

*2-(2,3-Dimethylphenoxy)-1-phenylethanamine (**38**).* ^{1}H NMR (300 MHz, $CDCl_3$): 7.50−7.47 (m, 2H), 7.42−7.28 (m, 3H), 7.03 (t, J = 7.7 Hz, 1H), 6.79 (d, J = 7.5 Hz, 1H), 6.68 (d, J = 8.0 Hz, 1H), 4.47 (dd, J = 7.7, 3.8 Hz, 1H), 4.13−3.95 (AB of ABX, J_{AB} = 9.1 Hz, 2H), 2.39 (broad s, 2H), 2.30. MS: 242.1 (MH^+).

*2-(2,4-Dimethylphenoxy)-1-phenylethan-1-amine (**39**).* ^{1}H NMR (300 MHz, CD_3OD): 7.42−7.60 (m, 5H), 6.94 (m, 2H), 6.80 (d, J = 8.1 Hz, 1H), 4.79 (dd, J = 4.9, 7.1 Hz, 1H), 4.22−4.36 (m, 2H), 2.23 (s, 3H), 2.24 (s, 3H). MS: 242.3 (MH^+).

*2-(3,4-Dimethylphenoxy)-1-phenylethan-1-amine (**40**).* ^{1}H NMR (300 MHz, CD_3OD): 7.42−7.58 (m, 5H), 7.03 (d, J = 8.2 Hz, 1H), 6.82 (d, J = 2.7 Hz, 1H), 6.73 (dd, J = 2.8, 8.2 Hz, 1H), 4.73 (dd, J = 4.2, 8.4 Hz, 1H), 4.18−4.37 (m, 2H), 2.24 (s, 3H), 2.19 (s, 3H). MS: 242.1 (MH^+).

*2-(Naphthalen-2-yloxy)-1-phenylethan-1-amine (**41**).* ^{1}H NMR (300 MHz, CD_3OD): 8.81−8.35 (m, 3H), 7.82 (dd, J = 16.8, 10.6 Hz, 3H), 7.63 (d, J = 6.5 Hz, 4H), 7.56−7.09 (m, 5H), 4.81 (s, 1H), 4.40 (s, 2H). MS: 264.1 (MH^+). R_f = 0.45 (5% methanol in dichloromethane on silica gel).

*2-(Naphthalen-1-yloxy)-1-phenylethan-1-amine (**42**).* ^{1}H NMR (300 MHz, DMSO-d_6): 8.8 (s, 3H), 8.44 (d, J = 9.6 Hz, 1H), 7.96−7.76 (m, 1H), 7.49 (m, 9H), 6.99 (d, J = 7.5 Hz, 1H), 4.9 (m, 1H), 4.46 (d, J = 5.7 Hz, 2H). MS: 264.1 (MH^+). R_f = 0.50 (5% methanol in dichloromethane on silica gel).

Synthesis of *N*-Alkylated Analogues via Reductive Amination. *1-(2,6-Dimethylphenoxy)-N-methylpropan-2-amine (**43**). Step 1: 1-(2,6-Dimethylphenoxy)propan-2-one.* To a solution of α-bromoacetone (3.17 g, 16.66 mmol) in 30 mL of DMF were added 3.10 g (25.4 mmol) of 2,6-dimethylphenol and 3.40 g (24.6 mmol) of potassium carbonate. The mixture was stirred at 21 °C for 20 h and then at 55 °C for an additional 2 h. The reaction mixture was poured on water and extracted with ether. The organic phase was washed (2 M sodium hydroxide, brine), dried over sodium sulfate, and concentrated under reduced pressure. Chromatography on silica gel using a gradient of ethyl acetate in hexanes afforded 1.01 g (34% yield) of the target ketone. ^{1}H NMR ($CDCl_3$): 7.04−6.94 (m, 3H), 4.37 (s, 2H), 2.38 (s, 3H,), 2.30 (s, 6H). R_f = 0.31 (10% diethyl ether in hexanes on silica gel).

*Step 2. 1-(2,6-Dimethylphenoxy)-N-methylpropan-2-amine (**43**).* Sodium cyanoborohydride (38 mg, 0.602 mmol) was added to a solution of methylamine hydrochloride (76.3 mg, 1.13 mmol) and 1-(2,6-dimethylphenoxy)propan-2-one (54.5 mg, 0.31 mmol) in ethanol (2.7 mL) at 21 °C. The reaction was heated at 90 °C in a microwave reactor for 1 h and stopped by dropwise addition of 10% (w/w) $Na_2CO_{3(aq)}$ until pH 9; then Celite was added, and the mixture was concentrated to dryness. Product-infused Celite was loaded onto a silica gel column and eluted using a gradient of methanol in dichloromethane to provide the title compound (22.6 mg, 38% yield) as a pale yellow oil that solidified over time. ^{1}H NMR ($CDCl_3$): 7.02−6.93 (m, 3H), 6.43 (broad s, 1H), 3.93 (m, 2H), 3.58 (m, 1H), 2.86 (s, 3H), 2.30 (s, 6H), 1.52 (d, J = 6.6 Hz, 3H) ppm. R_f = 0.23 (10% methanol in dichloromethane on silica gel).

The following compounds were synthesized by the same sequence as **43**:

*1-(2,6-Dimethylphenoxy)-N-ethylpropan-2-amine (**44**).* ^{1}H NMR (300 MHz, $CDCl_3$): 7.02−6.92 (m, 3H), 6.23 (broad s, 1H), 4.03−3.96 (AB of ABX, J_{AB} = 10.1 Hz, 2H), 3.61 (m, 1H), 3.24 (m, 2H), 2.30 (s, 6H), 1.51 (d, J = 6.9 Hz, 3H), 1.45 (t, J = 6.4 Hz, 3H). MS: 208.2 (MH^+). R_f = 0.19 (10% methanol in dichloromethane on silica gel).

*1-(2,6-Dimethylphenoxy)-N-propylpropan-2-amine (**45**).* ^{1}H NMR (300 MHz, $CDCl_3$): 7.03−6.90 (m, 3H), 3.70 (m, 2H), 3.17 (m, 1H), 2.82−2.62 (m, 2H), 2.50 (broad s, 1H), 2.31 (s, 6H), 1.62 (m, 2H), 1.28 (d, J = 6.6 Hz, 3H), 0.99 (t, J = 7.4 Hz, 3H). MS: 222.3 (MH^+). R_f = 0.24 (10% methanol in dichloromethane on silica gel).

*1-(2,6-Dimethylphenoxy)-N-butylpropan-2-amine (**46**).* ^{1}H NMR (300 MHz, $CDCl_3$): 7.02−6.91 (m, 3H), 4.21 (broad s, 1H), 3.83−3.73 (AB of ABX, J_{AB} = 9.6 Hz, 2H), 3.27 (m, 1H), 2.95−2.76 (m, 2H), 2.30 (s, 6H), 1.65 (m, 2H), 1.43 (m, 2H,), 1.28 (d, J = 6.6 Hz, 3H), 0.98 (t, J = 7.2 Hz, 3H). MS: 236.2 (MH^+). R_f = 0.31 (10% methanol in dichloromethane on silica gel).

*1-(2,6-Dimethylphenoxy)-N-butylpropan-2-amine (**47**).* ^{1}H NMR (300 MHz, $CDCl_3$): δ 7.02−6.89 (m, 3H), 3.76−3.67 (m, 2H), 3.59 (app t, J = 4.9 Hz, 2H), 3.40 (s, 3H), 3.22−3.12 (m, 2H), 3.01−2.85 (m, 2H), 2.54 (broad s, 1H), 2.31 (s, 6H,), 1.22 (d, J = 6.6 Hz, 3H). MS: 238.2 (MH^+). R_f = 0.36 (10% methanol in dichloromethane on silica gel).

*1-(2,6-Dimethylphenoxy)-N-phenylpropan-2-amine (**48**).* ^{1}H NMR (300 MHz, $CDCl_3$): 7.20 (t, J = 7.7 Hz, 2H), 7.00 (m, 2H), 6.92 (m, 1H), 6.75−6.69 (m, 3H), 4.13 (broad s, 1H), 3.89 (m, 1H), 3.85−3.80 (m, 2H), 2.27 (s, 6H), 1.47 (d, J = 6.6 Hz, 3H). MS: 256.2 (MH^+). R_f = 0.34 (20% ethyl acetate in hexane on silica gel).

*1-(2,6-Dimethylphenoxy)-N-benzylpropan-2-amine (**49**).* ^{1}H NMR (300 MHz, $CDCl_3$): 7.40−7.3 (m, 4H), 7.27 (m, 1H, overlapping with the solvent signal), 7.01 (m, 2H), 6.93 (m, 1H), 4.00−3.87 (AB quartet, J = 13.1 Hz, 2H), 3.77−3.69 (m, 2H), 3.20 (m, 1H), 2.29 (s, 6H), 1.22 (d, J = 6.0 Hz, 3H). MS: 270.2 (MH^+). R_f = 0.24 (5% methanol in dichloromethane on silica gel).

*1-(2,6-Dimethylphenoxy)-N-(2-phenylethyl)propan-2-amine (**50**).* ^{1}H NMR (300 MHz, $CDCl_3$): 7.31 (m, 2H), 7.26 (m, 2H, overlapping with the solvent signal), 7.22 (t, J = 7.1 Hz, 1H), 7.01 (m, 2H), 6.92 (m, 1H), 3.67 (m, 2H), 3.15 (m, 1H), 3.06 (m, 1H), 2.96−2.83 (m, 2H), 2.25 (s, 6H), 1.18 (d, J = 6.1 Hz, 3H). MS: 284.1 (MH^+). R_f = 0.25 (5% methanol in dichloromethane on silica gel).

*2-(2,3-Dimethylphenoxy)-N-methyl-1-phenylethanamine (**55**).* ^{1}H NMR (300 MHz, $CDCl_3$): 7.48−7.46 (m, 2H), 7.42−7.3 (m, 3H), 7.01 (t, J = 7.7 Hz, 1H), 6.78 (d, J = 7.4 Hz, 1H), 6.68 (d, J = 8.3 Hz, 1H), 4.02 (m, 3H), 2.42 (s, 3H), 2.29 (s, 3H), 2.18 (s, 3H). MS: 256.2 (MH^+). R_f = 0.33 (5% methanol in dichloromethane on silica gel).

*2-(2,3-Dimethylphenoxy)-N-ethyl-1-phenylethanamine (**56**).* ^{1}H NMR (300 MHz, $CDCl_3$): 7.49−7.46 (m, 2H), 7.41−7.29 (m, 3H), 7.01 (t, J = 8.0 Hz, 1H), 6.78 (d, J = 7.4 Hz, 1H), 6.68 (d, J = 8.3 Hz, 1H), 4.20 (app dd, J = 8.0, 4.7 Hz, 1H), 4.12−4.03 (m, 2H), 2.64 (q, J = 7.2 Hz, 2H), 2.29 (s, 3H), 2.17 (s, 3H), 1.17 (t, J = 7.1 Hz, 3H). MS: 270.3 (MH^+). R_f = 0.18 (4% methanol in dichloromethane on silica gel).

*2-(2,3-Dimethylphenoxy)-N-propyl-1-phenylethanamine (**57**).* ^{1}H NMR (300 MHz, $CDCl_3$): 7.50−7.46 (m, 2H), 7.42−7.29 (m, 3H), 7.03 (t, J = 7.7 Hz, 1H), 6.79 (d, J = 7.1 Hz, 1H), 6.68 (d, J = 8.0 Hz, 1H), 4.18 (app dd, J = 8.5, 4.1 Hz, 1H), 4.10−3.99 (m, 2H), 2.56 (t, J = 7.1 Hz, 2H), 2.30 (s, 3H), 2.19 (s, 3H), 1.58 (m, 2H), 0.96 (t, J = 7.7 Hz, 3H). MS: 284.2 (MH^+). R_f = 0.23 (2% methanol in dichloromethane on silica gel).

*2-(2,3-Dimethylphenoxy)-N-butyl-1-phenylethanamine (**58**).* ^{1}H NMR (300 MHz, $CDCl_3$): 7.49−7.46 (m, 2H), 7.41−7.29 (m, 3H), 7.02 (t, J = 8.0 Hz, 1H), 6.79 (d, J = 7.4 Hz, 1H), 6.67 (d, J = 8.0 Hz,

https://doi.org/10.1021/acs.jmedchem.0c01545
J. Med. Chem. 2021, 64, 5384−5403

1H), 4.17 (app dd, J = 8.2, 3.9 Hz, 1H), 4.10−3.99 (m, 2H), 2.59 (t, J = 6.9 Hz, 2H), 2.30 (s, 3H), 2.19 (s, 3H), 1.54 (m, 2H), 1.40 (m, 2H), 0.94 (t, J = 7.4 Hz, 3H). MS: 298.2 (MH^+). R_f = 0.25 (2% methanol in dichloromethane on silica gel).

*2-(2,3-Dimethylphenoxy)-N-methoxy-ethyl-1-phenylethanamine (**59**).* ^{1}H NMR (300 MHz, $CDCl_3$): 7.25 (s, 1H), 6.96−7.05 (m, 2H), 6.92 (dd, J = 6.2, 8.4 Hz, 1H), 4.14−4.31 (m, 1H), 3.58−3.79 (m, 2H), 2.29 (s, 6H), 1.27 (d, J = 6.5 Hz, 7H). MS: 300.1 (MH^+). ^{13}C NMR (125 MHz, CD_3OD): 157.22, 139.42, 133.80, 131.31, 130.69, 129.87, 124.84, 111.27, 69.93, 68.14, 63.04, 59.41, 49.32, 20.23. MS: 300.1 (MH^+). Calcd m/z for $[C_{19}H_{25}NO_2 + H^+]$: 300.1958. Observed: 300.1952.

*2-(3,5-Dimethylphenoxy)-N-(2-methoxyethyl)-1-phenylethan-1-amine (**60**).* ^{1}H NMR (300 MHz, CD_3OD) δ 7.22−7.47 (m, 5H), 6.49−6.61 (m, 3H), 3.96−4.13 (m, 2H), 3.33−3.56 (m, 2H), 3.35 (s, 3H), 2.53−2.76 (m, 1H), 2.24 (d, J = 0.7 Hz, 6H). MS: 300.1 (MH^+).

*2-(3,5-Bis(trifluoromethyl)phenoxy)-N-(2-methoxyethyl)-1-phenylethan-1-amine (**61**).* ^{1}H NMR (300 MHz, $CDCl_3$): 7.32−7.50 (m, 6H), 7.27 (d, J = 10.2 Hz, 2H), 4.08−4.21 (m, 4H), 3.50 (m, 1H), 3.38 (s, 3H), 2.62−2.85 (m, 2H). MS: 407.2 (MH^+).

*2-((2-(3,5-Dimethylphenoxy)-1-phenylethyl)amino)ethan-1-ol (**62**).* ^{1}H NMR (300 MHz, $CDCl_3$): 2.28 (s, 6H), 2.61−2.87 (m, 2H), 3.52−3.74 (m, 2H), 3.94−4.10 (m, 2H), 4.10−4.19 (m, 1H), 6.50−6.64 (m, 2H), 7.22−7.46 (m, 6H). MS: 286.2 (MH^+).

*2-((2-(3,5-Bis(trifluoromethyl)phenoxy)-1-phenylethyl)amino)-ethan-1-ol (**63**).* ^{1}H NMR (300 MHz, $CDCl_3$): 7.37−7.61 (m, 6H), 7.33 (d, J = 10.2 Hz, 2H), 4.08−4.21 (m, 4H), 3.50 (m, 1H), 2.62−2.85 (m, 2H). MS: 394.0 (MH^+).

Synthesis of Amide Analogues. *N-(1-(2,6-Dimethylphenoxy)-propan-2-yl)acetamide (**51**).* To 15 mg (0.06 mmol) of mexiletine hydrochloride and triethylamine (0.020 mL, 0.14 mmol) in dichloromethane (1 mL), acetyl chloride (0.006 mL, 0.08 mmol) was added. The mixture was stirred at 21 °C for 15 h, concentrated to dryness, and purified by flash chromatography (silica gel, ethyl acetate/hexane gradient) to afford 10.2 mg (65%) of **51**. ^{1}H NMR (300 MHz, $CDCl_3$): 6.86−7.08 (m, 3H), 5.93 (s, 1H), 4.28−4.44 (m, 1H), 3.66−3.86 (m, 2H), 2.26 (s, 6H), 2.04 (s, 3H), 1.41 (d, J = 6.8 Hz, 3H). MS: 222.2 (MH^+).

*N-(1-(2,6-Dimethylphenoxy)propan-2-yl)benzamide (**52**).* ^{1}H NMR (300 MHz, $CDCl_3$): 7.73−7.92 (m, 2H), 7.38−7.57 (m, 3H), 6.87−7.05 (m, 3H), 6.64 (d, J = 8.4 Hz, 1H), 4.57 (m, 1H), 3.95 (dd, J = 3.8, 9.1 Hz, 1H), 3.90 (s, 2H), 3.78−4.00 (m, 2H), 2.28 (s, 6H), 1.54 (d, J = 6.8 Hz, 3H). MS: 284.2 (MH^+).

*N-(2-(2,6-Dimethylphenoxy)-1-phenylethyl)acetamide (**53**).* ^{1}H NMR (300 MHz, $CDCl_3$): 7.29−7.43 (m, 4H), 6.87−6.98 (m, 3H), 6.39−6.43 (m, 1H), 5.33−5.39 (m, 1H), 3.98−4.10 (m, 2H), 2.11 (s, 6H). MS: 284.1 (MH^+).

*N-(2-(2,6-Dimethylphenoxy)-1-phenylethyl)benzamide (**54**).* ^{1}H NMR (300 MHz, $CDCl_3$): 7.84−7.88 (1H), 7.44−7.53 (m, 4H), 7.30−7.41 (m, 4H), 7.15−7.18 (m, 1H), 6.88−6.98 (m, 4H), 6.39−6.43 (m, 1H), 5.52−5.58 (m, 1H), 4.21 (dd, J = 4.4 and 9.4 Hz, 1H), 4.11 (dd, J = 3.9 and 9.4 Hz, 1H), 2.13 (s, 6H). MS: 346.0 (MH^+).

*(R)-1-Phenyl-2-(2-(trifluoromethyl)phenoxy)ethanamine (R)-**30**. Step 1: (R)-tert-Butyl 1-Phenyl-2-(2-(trifluoromethyl)phenoxy)-ethylcarbamate.* To sodium hydride (78 mg of 60% suspension in oil, 0.76 mmol) in DMF (5 mL) was added 299 mg of 2-trifluoromethylphenol (1.8 mmol). After ca. 5 min, 499 mg (1.7 mmol) (4*R*)-1,2,3-oxathiazolidine-3-carboxylic acid, 4-phenyl 1,1-dimethylethyl ester-2,2-dioxide[23] in DMF (1 mL) was added. The mixture was stirred at 21 °C for 16 h and diluted with water. The product was extracted with ethyl acetate. The organic phase was washed (1 M aqueous sodium hydroxide, water, and brine), dried (magnesium sulfate), and concentrated under reduced pressure. Purification of the residue afforded 587 mg (92% yield) of a colorless oil that was used without further characterization. R_f = 0.7 (30% ethyl acetate in hexanes on silica gel).

Step 2. To a solution of the precursor from Step 1 above (587 mg, 1.5 mmol) in methanol (10 mL) at 21 °C was added a solution of hydrogen chloride in ether (2 M, 2 mL, 4.0 mmol). After stirring for 16 h, the solvent and excess hydrogen chloride were removed under a stream of nitrogen and the solid obtained was vacuum dried at room temperature to afford 350 mg (72%) of (*R*)-**30**. ^{1}H NMR (300 MHz, DMSO-d_6) δ 8.58 (br. s., 3H), 7.51−8.05 (m, 4H), 7.37−7.51 (m, 2H), 7.32 (d, J = 8.53 Hz, 1H), 7.14 (t, J = 7.56 Hz, 1H), 4.72 (t, J = 6.05 Hz, 1H), 4.32−4.59 (m, 2H). MS: 282.0 (MH^+). $[\alpha]_{589}^{20}$ = −19.9° (c = 0.23; methanol). Chiral HPLC retention time: 10.22 min. R_f = 0.3 (5% methanol in dichloromethane on silica gel, weak UV activity, stains with ninhydrin) for the free base.

The following compounds were synthesized using the same sequence as (*R*)-**30** with appropriate modifications:

*(S)-1-Phenyl-2-(2-(trifluoromethyl)phenoxy)ethanamine (S)-**30**.* ^{1}H NMR (300 MHz, DMSO-d_6) δ 8.60 (br. s., 3H), 7.59 (dd, J = 7.84, 15.54 Hz, 4H), 7.36−7.51 (m, 3H), 7.32 (d, J = 8.53 Hz, 1H), 7.14 (t, J = 7.84 Hz, 1H), 4.73 (t, J = 6.05 Hz, 1H), 4.34−4.59 (m, 2H). MS: 282.0 (MH^+). $[\alpha]_{589}^{20}$ +20.2° (c = 0.24; methanol). Chiral HPLC retention time: 10.96 min. R_f = 0.3 (5% methanol in dichloromethane on silica gel, for the free base).

*(R)-1-Phenyl-2-(2-methylphenoxy)ethanamine (R)-**27**.* ^{1}H NMR (500 MHz, CD_3OD) 7.55−7.63 (m, 2H), 7.43−7.55 (m, 3H), 7.09−7.20 (m, 2H), 6.84−6.99 (m, 2H), 4.30−4.40 (m, 2H), 2.26 (s, 3H). MS: 228.0 (MH^+). $[\alpha]_{589}^{20}$ −25.4° (c = 0.22; methanol) Chiral HPLC retention time: 7.42 min.

*(S)-1-Phenyl-2-(2-methylphenoxy)ethanamine (S)-**27**.* ^{1}H NMR (500 MHz, CD_3OD) 7.54−7.61 (m, 2H), 7.42−7.54 (m, 3H), 7.06−7.19 (m, 2H), 6.82−6.99 (m, 2H), 4.28−4.43 (m, 2H), 2.26 (s, 3H). MS: 228.0 (MH^+). $[\alpha]_{589}^{20}$ +26.0° (c = 0.19; methanol). Chiral HPLC retention time: 8.34 min.

*(R)-2-(3,5-Dimethylphenoxy)-1-phenylethanamine (R)-**36**.* ^{1}H NMR (500 MHz, CD_3OD) 7.66−7.41 (m, 5H), 6.65 (s, 3H), 4.74 (dd, J = 8.4, 4.1 Hz, 1H), 4.35−4.25 (m, 2H), 2.27 (s, 6H). MS: 242.0 (MH^+). $[\alpha]_{589}^{20}$ −26.7° (c = 0.19, CD_3OD). Chiral HPLC retention time: 12.66 min. R_f = 0.42 (1:20 methanol/dichloromethane on silica gel).

*(S)-2-(3,5-Dimethylphenoxy)-1-phenylethanamine (S)-**36**.* ^{1}H NMR (500 MHz, CD_3OD) 7.93−7.15 (m, 5H), 6.65 (s, 3H), 4.74 (dd, J = 8.4, 4.1 Hz, 1H), 4.36−4.24 (m, 2H), 2.27 (s, 6H). MS: 242.0 (MH^+). $[\alpha]_{589}^{20}$ +28.2° (c = 0.1875, methanol). Chiral HPLC retention time: 9.71 min. R_f = 0.42 (1:20 methanol/dichloromethane).

Synthesis of (*R*)-59. *Step 1: (R)-N-(2-Hydroxy-1-phenylethyl)-2-methoxyacetamide.* Methoxyacetic acid (1.595 mL, 20.8 mmol) and EDCI (4.12 g 21.5 mmol) were added to a solution of (*R*)-phenylglycinol (3.17 g, 23.1 mmol) in dichloromethane (150 mL). The mixture was vigorously shaken to break the aggregates formed and then stirred at 21 °C for 5 h. After cooling to −20 °C and filtering through a Celite pad, the filtrate was concentrated under reduced pressure and purified by chromatography on silica gel using a methanol/dichloromethane gradient to give 750 mg of the *N*-(2-hydroxy-1-phenylethyl)-2-methoxyacetamide as an off-white solid that was used without characterization.

Step 2: (4R)-1,2,3-Oxathiazolidine-3-methoxyacetamido-4-phenyl-2,2-dioxide. A solution of imidazole (1.75 g, 25.6 mmol) and triethylamine (2.14 mL, 15.4 mmol) in dichloromethane (30 mL) was cooled to −60 °C. Thionyl chloride (0.56 mL, 7.69 mmol) was added dropwise. Temperature was kept at −60 to −50 °C. (*R*)-*N*-(2-Hydroxy-1-phenylethyl)-2-methoxyacetamide (1.34 g, 6.4 mmol) in dichloromethane (100 mL) was added dropwise over a period of 1 h. The mixture was stirred at −60 °C for an additional 3 h and then allowed to reach ambient temperature. After 20 min at 21 °C, water was added and the organic phase was separated. The organic layer was washed with brine, dried over sodium sulfate, and concentrated under reduced pressure. The residue was dissolved in 3:1 acetonitrile/water (100 mL) and cooled in an ice−water bath (4−5 °C). Sodium periodate (2.92 g, 13.6 mmol) was added followed by $RuCl_3(H_2O)_3$ (5 mg, 0.02 mmol). The mixture was stirred for 30 min and allowed to reach ambient temperature. More water was added to bring the acetonitrile/water ratio to 1:1. After stirring for an additional hour, the mixture was extracted with ether. The organic phase was washed with brine, dried over sodium sulfate, and concentrated under reduced pressure. The residue was purified by chromatography on silica gel using an ethyl acetate/hexane gradient to afford (4*R*)-1,2,3-

https://doi.org/10.1021/acs.jmedchem.0c01545
J. Med. Chem. 2021, 64, 5384−5403

oxathiazolidine-3-methoxyacetamido-4-phenyl-2,2-dioxide as a white solid. ^{1}H NMR (500 MHz, $CDCl_3$) δ 7.48−7.33 (m, 5H), 5.61 (dd, J = 7.1, 6.0 Hz, 1H), 5.02−4.86 (m, 1H), 4.53 (dd, J = 9.4, 5.9 Hz, 1H), 4.32 (dd, J = 33.6, 15.7 Hz, 2H), 3.42 (s, 3H). MS: 272.1 (MH^+). R_f = 0.43 (40% hexanes/EtOAc on silica gel).

Step 3: (R)-N-(2-(2,3-Dimethylphenoxy)-1-phenylethyl)-2-methoxyacetamide. 2,3-Dimethyl phenol (396 mg, 3.2 mmol) in DMF (10 mL) was treated with NaH, 60% dispersion in mineral oil (141 mg, 3.5 mmol), and stirred for 20 min. (*R*)-Cyclic sulfamidate (obtained in Step 2 above) (800 mg, 2.9 mmol) was added. The mixture was stirred for 4 h and partitioned between brine and ethyl acetate. The organic phase was washed with additional brine and dried over sodium sulfate. The solvent was removed *in vacuo*, and the crude product was purified on silica gel using an ethyl acetate/hexane gradient to afford 479 mg of (*R*)-*N*-(2-(2,3-dimethylphenoxy)-1-phenylethyl)-2-methoxyacetamide as a clear oil. ^{1}H NMR (300 MHz, $CDCl_3$) δ 7.22−7.49 (m, 5H), 7.04 (t, J = 7.98 Hz, 1H), 6.80 (d, J = 7.70 Hz, 1H), 6.68 (d, J = 8.25 Hz, 1H), 5.39−5.59 (m, 1H), 4.18−4.39 (m, 2H), 3.97 (s, 2H), 3.39−3.51 (m, 3H), 2.28 (s, 3H), 2.10−2.18 (m, 3H). MS: 314.2 (MH^+). R_f = 0.7 (19:1 dichloromethane/methanol on silica gel).

*Step 4: (R)-2-(2,3-Dimethylphenoxy)-N-(2-methoxyethyl)-1-phenylethanamine (R)-**59**.* To 479 mg (1.5 mmol) of (*R*)-*N*-(2-(2,3-dimethylphenoxy)-1-phenylethyl)-2-methoxyacetamide in 15 mL of anhydrous THF was added 1.0 M $LiAlH_4$ in THF (6.0 mL). The mixture was heated at 80 ° C for 24 h, cooled in an ice/water bath, and diluted with anhydrous THF. The excess reagent was neutralized by dropwise addition of H_2O (240 μL), dropwise addition of 3.5 M NaOH (240 μL), and further addition of H_2O (720 μL). After stirring for 10 min, magnesium sulfate was added; the mixture was allowed to reach ambient temperature and filtered through Celite. The filtrate was concentrated *in vacuo* and purified by chromatography on silica gel using a methanol/dichloromethane gradient. The amine was transferred to a vial using an appropriate amount of 0.5 M HCl in methanol. After thoroughly drying the product *in vacuo*, the desired HCl salt was obtained as a white powder. ^{1}H NMR (500 MHz, CD_3OD) δ 7.61 (dd, J = 7.7, 1.9 Hz, 2H), 7.58−7.45 (m, 3H), 7.04 (t, J = 7.9 Hz, 1H), 6.82 (t, J = 7.9 Hz, 2H), 4.88−4.83 (m, 1H), 4.48 (dd, J = 10.6, 7.1 Hz, 1H), 4.43−4.33 (m, 1H), 3.40 (s, 3H), 2.33−2.18 (m, 3H), 2.17 (s, 3H). MS: 300.1 (MH^+). $[\alpha]_{589}^{20}$ −25.1° (c = 0.278, methanol). Chiral HPLC retention time: 13.37 min. R_f = 0.45 (5% dichloromethane in methanol on silica gel).

(*S*)-**59** was prepared by the same route as (*R*)-**59** except that (*S*)-phenylglycinol was used as the starting material.

*(S)-2-(2,3-Dimethylphenoxy)-N-(2-methoxyethyl)-1-phenylethanamine (S)-**59**.* ^{1}H NMR (500 MHz, CD_3OD) δ 7.61 (dd, J = 7.7, 1.8 Hz, 2H), 7.57−7.48 (m, 3H), 7.04 (t, J = 7.9 Hz, 1H), 6.82 (t, J = 7.3 Hz, 2H), 4.49 (dd, J = 10.6, 7.1 Hz, 1H), 4.39 (dd, J = 10.6, 4.7 Hz, 1H), 3.77−3.57 (m, 1H), 3.40 (s, 3H), 2.26 (s, 3H), 2.15 (s, 3H). MS: 300.1 (MH^+). $[\alpha]_{589}^{20}$ +24.4° (c = 0.281, methanol). Chiral HPLC retention time: 14.17 min. R_f = 0.45 (5% dichloromethane: methanol on silica gel).

BIOLOGY EXPERIMENTAL SECTION

Cell Culture and Cell Differentiation to hiPSC-CMs. MyCell (LQTS3) and iCell (healthy individual) cardiomyocytes (Cellular Dynamics International, Madison, Wisconsin) were prepared as described previously.[30] Media were exchanged every other day by removing 50 μL of media and adding 50 μL of fresh iCCMM for 14 days prior to imaging. Human iPSCs were dissociated using 0.5 mM EDTA (ThermoFisher Scientific) in PBS without $CaCl_2$ or $MgCl_2$ (Corning) for 7 min at room temperature. Dissociated hiPSCs were plated at a density of 3 × 10^5 cells per well in a Matrigel coated 12-well plate in mTeSR1 media (StemCell Technologies) supplemented with 2 μM thiazovivin (Selleck Chemicals). After 24 h, the media were replaced with mTESR1 without thiazovivin and were replenished daily for 3−5 days until the cells reached ≥90% confluence to begin differentiation. Cardiomyocytes were differentiated by methods previously described.[29,30]

At day 25, cells were dissociated and plated onto Matrigel coated 384-well tissue culture plates (Greiner Bio-One) at a density of 20,000 cells/well. Experiments were conducted day 28 post-differentiation.

Preparation of VF2.1.Cl Loading Solution and Automated Image Acquisition. A VF2.1.Cl dye used was synthesized as described previously (Fluovolt, ThermoFisher).[31] One microliter of 2 mM VF2.1.Cl in DMSO was mixed with 1 μL of 10% Pluronic F127 (diluted in 1.7 mL water) by agitating and centrifuging three times. Separately, Hoechst 33258 was diluted into Tyrode's solution (136 mM NaCl, 5 mM KCl, 2 mM $CaCl_2$, 1 mM $MgCl_2$, 10 mM glucose, 10 mM HEPES, pH 7.4) to a concentration of 4 μg/mL. One milliliter of Hoechst/Tyrode's solution was added to a 1.7 mL VF2.1.Cl/Pluronic F127 mixture and mixed for 10 s. Each test compound was diluted in Tyrode's solution to a 2× concentrated stock and added to a well and incubated at 37 °C and 5% CO_2 for 5 min before image acquisition. Time series images were acquired automatically using a IC200 KIC instrument (Vala Sciences, San Diego, CA) at an acquisition frequency of 100 Hz for a duration of 6.5 s or 33 Hz for 20 s, with an excitation wavelength of 485/20 nm and emission filter of 525/30 nm using a 0.75 NA 20× Nikon Apo VC objective. A single image of the Hoechst/Tyrode solution was acquired after the time series. Optimized dye loading and imaging conditions were replicated using a different high content imager, the ImageXpress Micro XLS platform (Molecular Devices), and hiPSC-CMs produced by a novel differentiation protocol.[30]

Image Analysis, Physiological Parameter Calculations, and Data Analysis. Image analysis and physiological parameter calculations were conducted using Cyteseer (Vala Sciences) as previously described.[32,33] Briefly, an image output by a Cyteseer scanner was loaded into Cyteseer and a cardiac time series algorithm was executed on image files. Data were analyzed using Microsoft Excel 2013, and dose−response curves were calculated using GraphPad Prism 7 software (Prism, San Diego, CA).

Meta-Analysis of Experimental Data. An R-script (R version 3.3.1) was developed in-house that read CSV files generated by Cyteseer and amalgamated all the physiological parameters of interest into a single file. Using this dataset, meta-analysis of experimental data was conducted and showed intra- and intervariability in studies examining thawing cells in different ways (i.e., APD_{75}) and the relationship between APD_{75} and beat rate. Because of the nonlinear relationship of APD_{75} and beat rate, statistical significance was determined using a sliding window (center value ±3) to mirror experimental ranges. A Mann−Whitney test was applied to the data (using the Bonferroni criterion) for multiple testing.

Automated Patch Clamp Studies. Whole cell planar patch clamp recordings were used to study the effects of test compounds in transfected cells using ion channel currents including: I_{NaP}, I_{NaL}, and I_{Kr} channels.[34] For each compound studied, at least six increasing concentrations were included to obtain a dose−response relationship. For Na^+ channel experiments, a stable HEK cell line expressing a long QT mutant, F1473C,[35] was used. For I_{Kr}, a commercially available CHO stable cell line, hERG Duo (Bsys, Basel, Switzerland), was used. Cells were grown to ∼75% confluence, dissociated with trypsin−EDTA (Gibco, Waltham, MA), and resuspended in extracellular recording solutions at a density of ∼1 million cells/mL. Cells in solution were added to the Patchliner system (Nanion, Munich, DE) for voltage clamp recordings. The following solutions were used: internal solution for K^+ channel experiments: 50 mM KCl, 10 mM NaCl, 60 mM K-fluoride, 20 mM EGTA, and 10 mM HEPES/KOH, pH 7.2; internal solution for Na^+ channel experiments: 50 mM CsCl, 10 mM NaCl, 60 mM Cs-fluoride, 20 mM EGTA, 10 mM HEPES/CsOH, pH 7.2; external solutions for K^+ and Na^+ channel experiments; 140 mM NaCl, 4 mM KCl, 1 mM $MgCl_2$, 5 mM D-glucose monohydrate, and 10 mM HEPES/NaOH H 7.4. Test compounds (and controls) were prepared in extracellular solution with 0.01% DMSO. All reagents, unless otherwise noted, were obtained from Sigma-Aldrich (St. Louis, MO). Specific channel blockers tetrodotoxin (Calbiochem, San Diego, CA) and E-4031 were prepared in extracellular solution.

https://doi.org/10.1021/acs.jmedchem.0c01545
J. Med. Chem. 2021, 64, 5384−5403

Data Analysis. Normalized blocking ratio data, for each of I_{Kr}, I_{NaP}, and I_{NaL}, were fitted by a four parameter logistic fit. Patch clamp data were acquired with PatchMaster (HEKA, Lambrecht, DE) and PatchLiner Data acquisition (Nanion, Munich, DE) and analyzed with Origin 7.0 (OriginLab, Northampton, MA, USA), IgorPro (WaveMetrics, Portland, OR, USA), and MATLAB (Mathworks, Natick, MA, USA). Data were shown as mean ± SEM. Statistical data analyses were assessed with Student's *t*-test; differences at $P < 0.05$ were considered as statistically significant.

Data Analysis. Offline data analysis, curve fitting, and statistical evaluations were conducted with OriginPro 2016 (OriginLab, Northampton, MA) software. Dose−response curves for test compound inhibition were determined by measuring "peak" and "late" sodium current components on the same current trace. "Peak" values for the each response were defined automatically by the "negative peak searching" algorithm in OriginPro, whereas "late" component values were defined as an average of 20 ms of the current response after the current amplitude reached the steady-state level. Values for each test compound concentration were normalized to control currents recorded during the control solution applications. Dose−response data for each sodium current response component were fitted using a Marquardt−Levenberg iteration algorithm with a standard Hill equation. Data were presented as mean ± s.d.

Chemical Stability of Mexiletine Analogues at Various Temperatures and pHs. A typical chemical stability incubation contained 100 μM of the test compound prepared in 50 mM PBS buffer (pH 3.0 or 7.4,) with 1% ethanol. Test compounds were incubated at 37 °C. An aliquot from each incubation was taken at various times and injected onto an RP-HPLC. Samples were run on a Hitachi D-7000 HPLC system (Hitachi High Tech) using an L-7100 analytical pump, L-7400 UV−vis variable wavelength detector, and L-7600 automatic sample injector. A Gemini C18 column (250 × 4.6 mm, 5 μm particle size; Phenomenex) with a C18 guard column (Phenomenex) was used for chromatographic separation of mexiletine analogues. The mobile phase used was an isocratic system using 75% water (0.05% TFA) and 25% acetonitrile (0.05% TFA) with a flow rate of 1.25 mL/min and monitored at 275 nM. The disappearance of the analyte was monitored over time. A plot of the area under the curve for the normalized analyte versus time afforded the half-life values and k_{app}.

Metabolic Stability Studies in the Presence of Human Liver Microsomes and S-9. Human liver S-9, human liver microsomes, highly purified cytochrome P-450 (CYP) 3A4, 3A5, and 2D6, and NADPH-generating system were obtained from BD Biosciences (Waltham, MA). A typical incubation contained human liver microsomes or S-9 (0.4−0.5 and 1 mg of protein, respectively), 50 mM potassium phosphate buffer (pH 7.4), 50 μM test compound, an NADPH-generating system consisting of 0.5 mM $NADP^+$, 0.5 mM glucose-6-phosphate, 5 U/mL glucose-6-phosphate dehydrogenase, 1 mg/mL diethylenetriaminepentaacetic acid (DETAPAC), and 3 mM $MgCl_2$ in a final incubation volume of 0.25 mL. Incubations were run for 0, 7, 15, 30, and 60 min with constant shaking at 37 °C in a water bath and were terminated by addition of 0.75 mL of cold acetonitrile. After centrifugation at 3000 rpm for 5 min, the organic fraction was collected and solvent was removed with a stream of argon. The residue was reconstituted in 125 μL of MeOH and 125 μL of H_2O, mixed thoroughly, centrifuged at 13,000 rpm for 5 min, and analyzed by high-performance liquid chromatography. Samples were run on a Hitachi D-7000 HPLC system (Hitachi High Tech) as described above with a Gemini C18 column (250 × 4.6 mm, 5 μm particle size; Phenomenex) with a C18 guard column (Phenomenex). The mobile phase used was an isocratic system using 75% water (0.05% TFA) and 25% acetonitrile (0.05% TFA) with a flow rate of 1.25 mL/min and monitored at 275 nM. The disappearance of the analyte was monitored over time. A plot of the area under the curve for normalized analyte versus time afforded the half-life values and k_{app}.

***In Vivo* Effects of Mexiletine and Analogues.** Animal work followed the Guide for Care and Use of Animals as adopted by NIH. Formal approval was obtained from the IACUC of HBRI and UCLA. Animals used in the research studies were handled, housed, and killed in accordance with the current IACUC protocol and all applicable local, state, and federal regulations and guidelines.

Adult male Balb/C mice or Sprague Dawley rats (from Charles River, San Diego, CA) were housed in groups of four and maintained in a temperature-controlled environment on a 12 h:12 h light cycle (0600H on−1800H off) upon arrival to the laboratory. Animals were given free access to food and water during a 1 week habituation period to the laboratory. For PK studies, mexiletine and test compounds (in 0.9% saline) were administered to individually housed, starved jugular-cannulated Sprague Dawley rats (5 mg/kg i.v. or 25 mg/kg oral). At 10 time points over 25 h, blood was withdrawn, cooled, and centrifuged. Serum was combined with an internal standard (compound **44**), extracted with aqueous NaCl, Na_2CO_3, and ethyl acetate, separated, evaporated to dryness, taken up in methanol, and injected into the Agilent LCMS described above. Peak areas were quantified, and pharmacokinetic parameters were determined with a WinNonlin-Pro program (Pharsight, Inc., Princeton, NJ). For behavioral studies, test compounds or mexiletine were dissolved in DMSO (7%), PEG400 (57%) isotonic saline (40%), and administered i.p. to separate groups in a volume of 0.1 mL/mouse.

***Ex Vivo* Studies.** For *ex-vivo* studies, the effect of (*R*)-**30** on isolated heart tissue isolated from aged Sprague Dawley rats was examined. Vulnerability to EAD formation was investigated by examining the arrhythmogenic effects of hydrogen peroxide (H_2O_2) perfusion in isolated Langendorff rat hearts. Oxidative stress was shown to readily induce EADs at the isolated myocyte level in aged hearts from 24−26 month old rats. H_2O_2 exposure consistently promoted EADs and triggered activity in >90% of the aged fibrotic hearts that lead to VT/VF.

AUTHORSHIP CONTRIBUTIONS

J.R.C., K.O., D.R., R.S.K., H.S.K., and M.M. participated in the research design. J.R.C., D.R., J.G.-G., K.O., M.J., W.L.M., A.P., and K.S. conducted experiments. D.R., J.G.-G., K.O., and M.J. contributed new reagents or analytical tools. J.R.C., W.M., K.J.S., R.S.K., H.S.K., and M.M. performed data analysis. J.R.C., J.G.-G., R.S.K., W.L.M., and M.M. wrote or contributed to the writing of the manuscript.

ASSOCIATED CONTENT

Supporting Information

The Supporting Information is available free of charge at https://pubs.acs.org/doi/10.1021/acs.jmedchem.0c01545.

Molecular formula strings (CSV)

HPLC Methods and traces (PDF)

AUTHOR INFORMATION

Corresponding Author

John R. Cashman − *Human BioMolecular Research Institute, San Diego, California 92121, United States;* orcid.org/0000-0002-8628-9129; Phone: (858) 458-9305; Email: JCashman@HBRI.org; Fax: (858) 458-9311

Authors

Daniel Ryan − *Human BioMolecular Research Institute, San Diego, California 92121, United States*

Wesley L. McKeithan − *Cardiovascular Institute and Department of Medicine, Stanford University, Stanford, California 94305, United States; Graduate School of Biomedical Sciences, Sanford Burnham Prebys Medical Discovery Institute, San Diego, California 92037, United States*

Karl Okolotowicz − *Human BioMolecular Research Institute, San Diego, California 92121, United States*

https://doi.org/10.1021/acs.jmedchem.0c01545
J. Med. Chem. 2021, 64, 5384−5403

Jorge Gomez-Galeno − *Human BioMolecular Research Institute, San Diego, California 92121, United States*
Mark Johnson − *Human BioMolecular Research Institute, San Diego, California 92121, United States*
Kevin J. Sampson − *Department of Pharmacology, College of Physicians and Surgeons, Columbia University, New York 10032, United States*
Robert S. Kass − *Department of Pharmacology, College of Physicians and Surgeons, Columbia University, New York 10032, United States*
Arash Pezhouman − *Division of Cardiology, Department of Medicine, David Geffen School of Medicine, University of California Los Angeles, Los Angeles, California 90095, United States*
Hrayr S. Karagueuzian − *Division of Cardiology, Department of Medicine, David Geffen School of Medicine, University of California Los Angeles, Los Angeles, California 90095, United States*
Mark Mercola − *Cardiovascular Institute and Department of Medicine, Stanford University, Stanford, California 94305, United States; Graduate School of Biomedical Sciences, Sanford Burnham Prebys Medical Discovery Institute, San Diego, California 92037, United States*

Complete contact information is available at: https://pubs.acs.org/10.1021/acs.jmedchem.0c01545

Notes

The authors declare no competing financial interest.

■ ACKNOWLEDGMENTS

We are grateful for the financial support of the California Institute for Regenerative Medicine (CIRM) (Grant number TR4-06857 to J.R.C. and M.M.). The contents of this publication are solely the responsibility of the authors and do not necessarily represent the official views of CIRM or any other agency of the State of California. Flow cytometry and high-throughput screening services were supported by NIH P30CA030199 at the Sanford-Burnham-Prebys Medical Discovery Institute. We are grateful to Dr. Jim Weiss (UCLA) for help with the data of Figure 4. Some HPLC traces were done at AxisPharm, San Diego, CA, 92121.

■ ABBREVIATIONS

APD, action potential duration; AUC, area under the curve; *F*, bioavailability; CF, conduction velocity; C_{max}, concentration max; EADs, early after depolarizations; hERG, human ether-à-go-go; iPSC-CMs, induced pluripotent stem cell-derived cardiomyocytes; I_{Kr}, potassium current; ERG, inward potassium channel; KIC, kinetic image cytometry; I_{NaL}, late inward sodium current; LQTS3, long QT syndrome Type 3; I_{NaP}, peak sodium current; PK, pharmacokinetics; SAR, structure−activity relationship; TTX, tetradotoxin; VT, ventricular tachycardia; VF, ventricular fibrillation

■ REFERENCES

(1) Wu, E. Q.; Birnbaum, H. G.; Mareva, M.; Tuttle, E.; Castor, A. R.; Jackman, W.; Ruskin, J. Economic burden and co-morbidities of atrial fibrillation in a privately insured population. *Curr. Med. Res. Opin.* **2005**, *21*, 1693−1699.
(2) Zheng, Z. J.; Croft, J. B.; Giles, W. H.; Mensah, G. A. Sudden cardiac death in the United States, 1989 to 1998. *Circulation* **2001**, *104*, 2158−2163.
(3) Koplan, B. A.; Stevenson, W. G. Ventricular tachycardia and sudden cardiac death. *Mayo Clin. Proc.* **2009**, *84*, 289−297.
(4) Singh, S.; Kerndt, C.; Zeltser, R. *Mexiletine*; StatPearls: Treasure Island (FL), 2020.
(5) Al-Khatib, S. M.; Stevenson, W. G.; Ackerman, M. J.; Bryant, W. J.; Callans, D. J.; Curtis, A. B.; Deal, B. J.; Dickfeld, T.; Field, M. E.; Fonarow, G. C.; Gillis, A. M.; Granger, C. B.; Hammill, S. C.; Hlatky, M. A.; Joglar, J. A.; Kay, G. N.; Matlock, D. D.; Myerburg, R. J.; Page, R. L. 2017 AHA/ACC/HRS guideline for management of patients with ventricular arrhythmias and the prevention of sudden cardiac death: A report of the American college of cardiology/American heart association task force on clinical practice guidelines and the heart rhythm society. *Heart Rhythm.* **2017**, *15*, e190−e252.
(6) Priori, S. G.; Blomstrom-Lundqvist, C.; Mazzanti, A.; Blom, N.; Borggrefe, M.; Camm, J.; Elliott, P. M.; Fitzsimons, D.; Hatala, R.; Hindricks, G.; Kirchhof, P.; Kjeldsen, K.; Kuck, K. H.; Hernandez-Madrid, A.; Nikolaou, N.; Norekval, T. M.; Spaulding, C.; Van Veldhuisen, D. J.; ESC Scientific Document Group. 2015 ESC guidelines for the management of patients with ventricular arrhythmias and the prevention of sudden cardiac death: The task force for the management of patients with ventricular arrhythmias and the prevention of sudden cardiac death of the European society of cardiology (ESC). Endorsed by: Association for European paediatric and congenital cardiology (AEPC). *Eur Heart J.* **2015**, *36*, 2793−2867.
(7) Bennett, P. B.; Yazawa, K.; Makita, N.; George, A. L., Jr. Molecular mechanism for an inherited cardiac arrhythmia. *Nature* **1995**, *376*, 683−685.
(8) Wang, Q.; Shen, J.; Splawski, I.; Atkinson, D.; Li, Z.; Robinson, J. L.; Moss, A. J.; Towbin, J. A.; Keating, M. T. SCN5A mutations associated with an inherited cardiac arrhythmia, long QT syndrome. *Cell* **1995**, *80*, 805−811.
(9) Wang, Q.; Shen, J.; Li, Z.; Timothy, K.; Vincent, G. M.; Priori, S. G.; Schwartz, P. J.; Keating, M. T. Cardiac sodium channel mutations in patients with long QT syndrome, an inherited cardiac arrhythmia. *Hum. Mol. Genet.* **1995**, *4*, 1603−1607.
(10) Moss, A. J.; Kass, R. S. Long QT syndrome: from channels to cardiac arrhythmias. *J. Clin. Invest.* **2005**, *115*, 2018−2024.
(11) Schwartz, P. J.; Priori, S. G.; Locati, E. H.; Napolitano, C.; Cantù, F.; Towbin, J. A.; Keating, M. T.; Hammoude, H.; Brown, A. M.; Chen, L.-S. K.; Colatsky, T. J. Long QT syndrome patients with mutations of the SCN5A and HERG genes have differential responses to Na^+ channel blockade and to increases in heart rate: Implications for gene-specific therapy. *Circulation* **1995**, *92*, 3381−3386.
(12) Mazzanti, A.; Maragna, R.; Faragli, A.; Monteforte, N.; Bloise, R.; Memmi, M.; Novelli, V.; Baiardi, P.; Bagnardi, V.; Etheridge, S. P.; Napolitano, C.; Priori, S. G. Gene-specific therapy with mexiletine reduces arrhythmic events in patients with long QT syndrome type 3. *J. Am. Coll. Cardiol.* **2016**, *67*, 1053−1058.
(13) McKeithan, W. L.; Savchenko, A.; Yu, M. S.; Cerignoli, F.; Bruyneel, A. A. N.; Price, J. H.; Colas, A. R.; Miller, E. W.; Cashman, J. R.; Mercola, M. An automated platform for assessment of congenital and drug-induced arrhythmia with hiPSC-derived cardiomyocytes. *Front. Physiol.* **2017**, *8*, 766.
(14) Gualdani, R.; Tadini-Buoninsegni, F.; Roselli, M.; Defrenza, I.; Contino, M.; Colabufo, N. A.; Lentini, G. Inhibition of hERG potassium channel by the antiarrhythmic agent mexiletine and its metabolite *m*-hydroxymexiletine. *Pharmacol. Res. Perspect.* **2015**, *3*, No. e00160.
(15) Campbell, N. P.; Kelly, J. G.; Adgey, A. A.; Shanks, R. G. The clinical pharmacology of mexiletine. *Br. J. Clin. Pharmacol.* **1978**, *6*, 103−108.
(16) Rudel, R.; Lehamann, H. F.; Ricker, K. The nondystrophic myotonias. In *Myology*, Chapt 49; Engel, A. G.; Franzini-Armstrong, C., eds; pp 1291−1302, McGraw-Hill: New York 1994.
(17) Terrenoire, C.; Wang, K.; Tung, K. W. C.; Chung, W. K.; Pass, R. H.; Lu, J. T.; Jean, J.-C.; Omari, A.; Sampson, K. J.; Kotton, D. N.; Keller, G.; Kass, R. S. Induced pluripotent stem cells used to reveal

drug actions in a long QT syndrome family with complex genetics. *J. Gen. Physiol.* **2013**, *141*, 61−72.
(18) De Bellis, M.; De Luca, A.; Desaphy, J. F.; Carbonara, R.; Heiny, J. A.; Kennedy, A.; Carocci, A.; Cavalluzzi, M. M.; Lentini, G.; Franchini, C.; Camerino, D. C. Combined modifications of mexiletine pharmacophores for new lead blockers of Na(v)1.4 channels. *Biophys. J.* **2013**, *104*, 344−354.
(19) De Luca, A.; Natuzzi, F.; Desaphy, J. F.; Loni, G.; Lentini, G.; Franchini, C.; Tortorella, V.; Camerino, D. C. Molecular determinants of mexiletine structure for potent and use-dependent block of skeletal muscle sodium channels. *Mol. Pharmacol.* **2000**, *57*, 268−277.
(20) Huang, P.-Q.; Zheng, X.; Wei, H. Synthesis of (*S*)-vasicol and (*S*)-3-hydroxy-2-pyrrolidinone. *Heterocycles* **2003**, *60*, 1833−1841.
(21) Huang, K.; Ortiz-Marciales, M.; Stepanenko, V.; De Jesús, M.; Correa, W. A Practical and efficient route for the highly enantioselective synthesis of mexiletine analogues and novel beta-thiophenoxy and pyridyl ethers. *J. Org. Chem.* **2008**, *73*, 6928−6931.
(22) Giardinà, D.; Crucianelli, M.; Angeli, P.; Buccioni, M.; Gulini, U.; Marucci, G.; Sagratini, G.; Melchiorre, C. Structure-activity relationships among novel phenoxybenzamine-related beta-chloroethylamines. *Bioorg. Med. Chem.* **2002**, *10*, 1291−1303.
(23) Kang, S.; Han, J.; Lee, E. S.; Choi, E. B.; Lee, H. K. Enantioselective synthesis of cyclic sulfamidates by using chiral rhodium-catalyzed asymmetric transfer hydrogenation. *Org. Lett.* **2010**, *12*, 4184−4187.
(24) Wang, D. W.; Kiyosue, T.; Sato, T.; Arita, M. Comparison of the effects of class I anti-arrhythmic drugs, cibenzoline, mexiletine and flecainide, on the delayed rectifier K^+ current of guinea-pig ventricular myocytes. *J. Mol. Cell. Cardiol.* **1996**, *28*, 893−903.
(25) Fenster, P. E.; Comess, K. A. Pharmacology and clinical use of mexiletine. *Pharmacotherapy* **1986**, *6*, 1−7.
(26) Alexander, G. J.; Kopeloff, L. M.; Alexander, R. B.; Chatterjie, N. Mexiletine: biphasic action on convulsive seizures in rodents. *Neurobehav. Toxicol. Teratol.* **1986**, *8*, 231−235.
(27) Akıncı, E.; Yüzbaşioglu, Y.; Coşkun, F. Hemodialysis as an alternative treatment of mexiletine intoxication. *Am. J. Emerg. Med.* **2011**, *29*, 1235−1235.e6.
(28) Karagueuzian, H. S.; Pezhouman, A.; Angelini, M.; Olcese, R. Enhanced late Na and Ca currents as effective antiarrhythmic drug targets. *Front. Pharmacol.* **2017**, *8*, 36.
(29) Burridge, P. W.; Matsa, E.; Shukla, P.; Lin, Z. C.; Churko, J. M.; Ebert, A. D.; Lan, F.; Diecke, S.; Huber, B.; Mordwinkin, N. M.; Plews, J. R.; Abilez, O. J.; Cui, B.; Gold, J. D.; Wu, J. C. Chemically defined generation of human cardiomyocytes. *Nat. Methods* **2014**, *11*, 855−860.
(30) Cunningham, T. J.; Yu, M. S.; McKeithan, W. L.; Spiering, S.; Carrette, F.; Huang, C. T.; Bushway, P. J.; Tierney, M.; Albini, S.; Giacca, M.; Mano, M.; Puri, P. L.; Sacco, A.; Ruiz-Lozano, P.; Riou, J. F.; Umbhauer, M.; Duester, G.; Mercola, M.; Colas, A. R. Id genes are essential for early heart formation. *Genes Dev.* **2017**, *31*, 1325−1338.
(31) Miller, E. W. Small molecule fluorescent voltage indicators for studying membrane potential. *Curr. Opin. Chem. Biol.* **2016**, *33*, 74−80.
(32) Cerignoli, F.; Charlot, D.; Whittaker, R.; Ingermanson, R.; Gehalot, P.; Savchenko, A.; Gallacher, D. J.; Towart, R.; Price, J. H.; McDonough, P. M.; Mercola, M. High throughput measurement of Ca^{2+} dynamics for drug risk assessment in human stem cell-derived cardiomyocytes by kinetic image cytometry. *J. Pharmacol. Toxicol. Methods* **2012**, *66*, 246−256.
(33) Lu, H. R.; Whittaker, R.; Price, J. H.; Vega, R.; Pfeiffer, E. R.; Cerignoli, F.; Towart, R.; Gallacher, D. J. High throughput measurement of Ca^{++} dynamics in human stem cell-derived cardiomyocytes by kinetic image cytometery: A cardiac risk assessment characterization using a large panel of cardioactive and inactive compounds. *Toxicol. Sci.* **2015**, *148*, 503−516.
(34) Farre, C.; Fertig, N. HTS techniques for patch clamp-based ion channel screening - advances and economy. *Expert. Opin. Drug. Discovery* **2012**, *7*, 515−524.
(35) Bankston, J. R.; Yue, M.; Chung, W.; Spyres, M.; Pass, R. H.; Silver, E.; Sampson, K. J.; Kass, R. S. A novel and lethal de novo LQT-3 mutation in a newborn with distinct molecular pharmacology and therapeutic response. *PLoS One* **2007**, *2*, No. e1258.

https://doi.org/10.1021/acs.jmedchem.0c01545
J. Med. Chem. 2021, 64, 5384−5403